STUDY OF NATURAL CONVECTION FROM CYLINDRICAL SURFACES EMBEDDED IN POROUS MEDIA BY LDCT

By
Mubarak A. Al-Khater
Department of Chemical Engineering

January 2004

Dedicated to

My Loving Parents, My Brothers, My Sisters,

Uncle Mansour and Uncle Mohammed

ACKNOWLEDGEMENT

Acknowledgement is due to King Fahd University of Petroleum & Minerals for providing me with this opportunity of research to purse my graduate degree. I am indebted to the Department of Chemical Engineering in KFUPM. The facilities and support of the Department made my work easier.

I am thankful to my Thesis Advisor Dr. Salim Ur-Rahman. He was always there to assist and support. I have learned so much working with him. I am also thankful to committee members from KFUPM, Professor Halim H. Redhwi, Dr. Mohammed Abul-Hamayel and Dr. Nadhir A. Al-Baghli. Special thanks are due to Dr. Maher Al-Odan, committee member from King Saud University in Riyadh who has provided viable comments and traveled a long distance to attend my thesis defense. Their constructive criticism helped in focusing my work better. I am also thankful to Kamal Mahjoob, Mariano Gica, Bashir Ahmad, Sayed Kamal Ahmad and Al Tares for their cooperation.

Special thanks to my mother for her prayers and support during this work. My brothers, Salah, Raed, Ali and Salah Al-Shammary, as well as my sisters were always there for me and have encourage me during my entire course of study at KFUPM.

My friends Abdullah Al-Muhaish, Adel Al-Bassam, Talal Al-Hareky and Chris Rudie were always encouraging.

My friends at KFUPM were always supportive. Rizwan Khan, Saifuddin Sheikh, Rehan Chaudhry, Nabil Abu-Ghandar and Sarfraz Abbasi and the graduate students in the Chemical Engineering Department.

TABLE OF CONTENTS

LIST OF FIGURES

LIST OF TABLES

THESIS ABSTRACT (ARABIC)

uü‘rT‘?R‘“Rrÿ“?‘ur‘?“ ?‘U‘?Œ

?Œ?Y?Œ

uÁ?Á»UŠrÁ»?Á rÁSÁtÁ?Œ

r?œ??rUt?? u UTr?Œ

?W uWWWtWfWVWV

?ä?Ÿ?R?ž u?s?Šr?R?Šut×

ÐtrŸ??R¿?us??t?ž??R?rŸ?rŠ

THESIS ABSTRACT

Name: MUBARAK A. AL-KHATER

Title: Study of Natural Convection from Cylindrical Surfaces Embedded in Porous Media by LDCT

Degree: MASTER OF SCIENCE

Major Field: CHEMICAL ENGINEERING

Date of Degree: January 2004

Natural convective mass transfer coefficients from vertical cylinders of varying aspect ratio, embedded in saturated porous media, were measured using limiting diffusion current technique (LDCT). Randomly packed glass spheres of different size formed the porous media. The obtained data are correlated in terms of modified Sherwood (Sh^*_L), modified Rayleigh number (Ra^*_L) and Darcy numbers (Da_L). For cylinders embedded in porous media, the mass transfer coefficients can be estimated using the following:

$Sh^*_L = 3.29\left(\frac{Ra^*_L}{Da_L}\right)^{0.26} * \left[1 + \frac{0.6L}{R}(Ra^*_L)^{-0.5}\right]$ in the range $6\times10^4 < Ra_L^* < 6.1\times10^6$ and $1.40 \times 10^{-6} < Da_L < 1.02 \times 10^{-3}$.

Master of Science Degree

King Fahd University of Petroleum & Minerals

Dhahran, Saudi Arabia

CHAPTER 1

INTRODUCTION

1.1. Background

The study of natural convection in porous media has been a focus of many researchers in the field of petroleum and chemical engineering. Many applications have been attributed to this research including petroleum reservoir engineering, thermal insulation of buildings and process equipment, storage of heat-generating materials like grains, catalysts, coal, etc., nuclear waste disposal, electronics applications and geophysical applications. Although many have contributed to theoretical studies in natural convection in porous media, only a few experimental studies exist. Even less experimental studies exist in problems involving cylindrical and conical objects. [1, 2, 3]

The average mass transfer coefficients can be obtained by limiting diffusion current technique (LDCT). The surface on which mass transfer coefficients are to be determined is made an electrode, associated with proper reference and counter electrodes and kept in a suitable electrolyte to form an electrochemical cell. Detailed description of LDCT is given in this chapter. This technique has advantages over the others because of its (a) simplicity (b) accuracy and (c) speed at which the experiments are performed. Local heat transfer coefficient, for example, can be estimated by using thermocouples and obtaining the temperature profile along the surface on which the transfer coefficient is desired. This method, however, requires a sophisticated experimental setup and does not ensure accurate data because the presence of the thermocouples modifies the boundary layer. Inferometers can also be used to determine the heat transfer coefficients, but this is difficult to use in case of surfaces embedded in porous media. Mass transfer coefficient can be obtained by measuring the rate of dissolution of a surface in fluid or in a saturated medium, but this produces less accurate data. This is mainly because of the surface shape changes during the process of dissolution causing the geometry to alter. Also, long waiting time is required in order to obtain appreciable dissolution rate. [4, 5]

This work is aimed at obtaining natural convective mass transfer coefficients from cylindrical surfaces embedded in saturated porous media. The obtained data will be used to deduce empirical models for Sherwood numbers of these situations.

1.2. Literature Review

1.2.1. Limiting Diffusion Current Technique

An electrochemical reaction, such as deposition of copper from acidified copper sulfate solution, involves essentially two steps. In the first step, ions are convected naturally or forced to the surface of the electrode. The second step is the actual electrochemical reaction that converts ions into metal. The first step is the mass transfer of the ions and it depends on the hydrodynamics and diffusion of the ions into the electrolyte. The second step is purely kinetic and depends on the applied potential and intrinsic kinetic fundamentals of the elemental reaction. The kinetic parameters, in turn depend on the temperature. When the applied potential is increased, the rate of electrochemical reaction increases. The overall rate of reaction (that includes mass transfer) becomes mass transfer limited as the rate of reaction becomes very fast. The rate of the reaction can now be written as:

$$N_A = k_L (C_b - C_s) = \frac{I_L}{AzF} \tag{1}$$

where,

I_L = The limiting current

A = Area of the electrode

z = charge number of the species

F = Faraday's constant

k_L = Mass transfer coefficient

C_b and C_s are the copper ion concentrations at the bulk and the surface respectively.

At this limiting condition, the concentration of the ions at the surface is essentially zero and Equation (1) becomes:

$$k = \frac{I_L}{AzFC_b} \tag{2}$$

Equation (2) is used to calculate mass transfer coefficient at any surface for a given hydrodynamic situation. It requires construction of cell of desired hydrodynamics and measurement of the limiting current. The limiting current can be obtained by carrying out a linear polarization experiment.

The mass flux in an electrochemical system is given by:

$$N_A = -zuFC_A\nabla \quad - D_A\nabla C_A + vC_A \tag{3}$$

where;

C_A = Concentration of the ion

v = Velocity of the fluid

= Applied potential

u = Mobility of ions

The concentration profiles can be obtained by solving Equation (3) with the mass balance equation, continuity equation and Navier-Stokes equation. The last two terms in Equation (3) are due to diffusion and bulk motion and corresponds to any non-electrolytic system. However, the first term is a result of the migration of ions by the presence of an electric field. The mass transfer coefficient estimated by Equation (2) will have effect of migration, if experimental conditions are not carefully chosen to exclude this effect. This could be done by increasing the conductivity of the electrolyte through increasing concentration of supporting electrolyte. This means ∇ will be negligible.

Newman [5] studied the effects of migration on limiting current and produced data for different concentration ratio $r_1 = C(H^+)/2C(SO_4^{2-})$. The ratio (Limiting Current Considering Migration)/ (Limiting Current Neglecting Migration) was plotted against $\sqrt{r_1}$ at various concentrations of solution. Using Newman's [5] results, the minimum concentration of the supporting electrolyte to produce negligible migration of ions can be estimated. It gives $\sqrt{r_1}$ = 0.99. For example, if the concentration of copper ions is 0.0529 M, the solution should contain at least 2.46 M sulfuric acid to avoid any migration effect. [4, 5]

There are some options available for reaction systems used in electrochemical mass transfer studies. The following are examples of model reactions used [4]:

$Cd^{2+} + 2e$?¶ Cd (4)

$Cu^{2+} + 2e$?ÙCu (5)

$Fe(CN)^{3-}_{6} + e$?ü $Fe(CN)^{4-}_{6}$ (6)

For studies of convection mass transfer, the copper deposition reaction is preferred for the following advantages: (a) $CuSO_4$ has a relatively high solubility at room temperature; (b) the electrode reaction does not produce a soluble product species and (c) the limiting current plateau is very well defined in this system. Deposition of copper from moderately concentrated solutions results in large density differences between bulk and surface solution resulting in large driving forces for natural convection. [6]

Wragg [7] referred to a problematic aspect of using a metal deposition process in LDCT work as is the case of using copper systems. Scan rate has a major effect on the value obtained for the limiting current. Very slow scan rate results into surface roughening of electrode and hence incorrect steady state values will be obtained. In very fast scan rates, on the other hand, limiting currents are detected in their transition to steady state values and hence incorrect values obtained. This illustrates that scan rates in metal deposition experiments must carefully be selected to obtain accurate values for the limiting currents. The use of dilute electrolyte is also detrimental to avoid the roughening problem. Ponce-de-Leon and Field [8] developed a technique to determine the limiting diffusion current when the plot of normalized resistance against the reciprocal of current does not exhibit well defined plateau. This work establishes the limiting current, for the absence of a clearly defined plateau, using E/I against 1/I plot. It uses a prescribed procedure to extract the value of limiting current.

1.2.2. Natural Convection from Plane Vertical Surfaces Embedded in Porous Media

Natural convection about a heated vertical surface placed in porous media was studied by Cheng and Minkowycz [9] where they obtained similarity solutions based on Darcy's law and boundary layer approximations for the case of constant discharge velocity of injection water and uniform temperature. Forr an arbitrary temperature profile given by:

$$T_w = T_{8ã} + Ax^{?ã} \qquad (7)$$

where; T_w = Temperature at the wall or surface, $T_{8ã}$ = Temperature far from the surface, A and λ are constants, the local heat flux at the heated plate is given by :

$$q'' = -k\left(\frac{\partial T}{\partial y}\right)_{y=0} = kA^{3/2}\left(\frac{g\ \ K}{v\alpha_m}\right)^{1/2} x^{(3\lambda-1)/2}\left[-\theta'(0)\right] \qquad (8)$$

In this equation:

ßÅ= Thermal expansion coefficient

a$_m$Q = Thermal diffusivity for porous media

$$\theta = \frac{T - T_\infty}{T_w - T_\infty}$$

g = acceleration of gravity

x = vertical length

v = average velocity parallel to surface

Table 1 shows the values of ?¶(0) at different values of ?¶ The case of ?¶=0 corresponds to a constant wall temperature which is analogous to the constant concentration in mass transfer. For ?ü=0, ?ű(0)=0.444, which can be substituted in Equation (8).

Cheng and Hsu [10] and Joshi and Gebhart [11] examined higher order effects to extend the applicability range of the boundary-layer analysis. A number of studies have considered various non-Daracian effects on the same problem. Bejan and Poulikakos [12] and Plumb and Huenefeld [13] used Forchheimer's equation to include inertia effects. Hsu and Cheng [14] and Evan and Plumb [15] studied boundary effects on heat transfer based on Brinkman's equation. They found good agreement with Cheng and Mickowycz theory for $Ra_x < 400$. Kim and Vafai [16] employed Brinkman-extended Darcy model. Cheng, Ali and Verma [17] used 3-mm glass packing and observed reasonable match with theory for $Ra_x<300$. Kaviany and Mittal [18, 19] preformed experiments with high permeability polyurethane foams with air. Most of their data are in agreement with their theory based on Brinkman-Forschheimer formulation. In their experiments, inertial effects are not significant because Rayleigh numbers are not high.

Table 1: Values of -?≯(0) for various values of ?≯for the heated vertical plate problem

(Cheng and Minkowycz [9])

?l	**-?I(0)**	
-1/3	0	
-1/4	0.162	
0	0.444	isothermal
1/4	0.630	
1/3	0.678	uniform flux
1/2	0.761	
3/4	0.892	
1	1.001	

Rahman, et al. [20] have obtained mass transfer coefficients from vertical surfaces embedded in various packing sizes of glass spheres of 16, 6, 4 and 3 mm diameter as well as beach sand. Rayleigh numbers in this study were high. They have compared their data with available models and observed that Bejan-Poulikakos model based on Forschheimer's equation matches the experimental observation. They produced the following model for the glass packing material:

$$Sh_L^* = 3.32\left(\frac{Ra_L^*}{Da_L}\right)^{0.26} \tag{9}$$

where;

$$Sh_L^* = \frac{k_L D}{D_e}$$

$$Ra_L^* = \frac{gKL(\quad / \quad_\infty - 1)}{vD_e}$$

$$Da = \frac{K}{\varepsilon L^2}$$

$$D_e = \frac{D\varepsilon}{\quad}$$

D = Molecular diffusivity of cupric ions in acidic solution

L = Hight of the plate

$e\varepsilon$= Porosity

t = Tortuousity of the porous media

v = Kinematic viscosity

1.2.3. Natural Convection from Embedded Vertical Cylinders

Minkowycz and Cheng [21] gave an approximate solution for heat transfer in the case of vertical cylinders embedded in porous media. The following equations describe the problem of steady natural convection about a vertical cylinder of radius R embedded in a saturated porous medium with a prescribed wall temperature.

$$\frac{\partial}{\partial r}(rv)+\frac{\partial}{\partial x}(ru)=0 \tag{10}$$

$$u=-\frac{K}{\mu}\left(\frac{\partial p}{\partial x}+?g\right) \tag{11}$$

$$v=-\frac{K}{\mu}\frac{\partial p}{\partial r} \tag{12}$$

$$u\frac{\partial T}{\partial x}+v\frac{\partial T}{\partial r}=\alpha\left[\frac{1}{r}\frac{\partial}{\partial r}\left(r\frac{\partial T}{\partial r}\right)+\frac{\partial^2 T}{\partial x^2}\right] \tag{13}$$

$$= \quad {}_{\infty}[1- \quad (T-T_{\infty})] \tag{14}$$

The boundary conditions for this problem are:

$$v=0, T=T_w \quad \text{at } r=R \tag{15}$$

$$u \to 0, T \to T_{\infty} \quad \text{at } r=\infty \tag{16}$$

For the case of constant wall temperature, the ratio of the local surface heat flux for a cylinder ($q_c^{"}$) to that of a vertical plate ($q^{"}$) is given by:

$$\frac{q_c^{"}}{q^{"}}=\frac{\left[-\theta'(\xi,0,\lambda)\right]}{\left[-\theta'(0,\lambda)\right]} \tag{17}$$

where curvature parameter ?3and $q^{"}$ are defined as:

$$\xi = \frac{2x}{R}\frac{1}{(Ra*_x)^{1/2}} \tag{18}$$

and the local heat flux from flat vertical surface is :

$$q'' = -k\left(\frac{\partial T}{\partial y}\right)_{y=0} = kA^{3/2}\left(\frac{g\ k}{\alpha_m}\right)^{1/2} x^{(3\lambda-1)/2}\left[-?I(0)\right] \tag{19}$$

Here, -?ð(0) is 0.444 for the constant temperature case (λ = 0) as shown in Table 1. Table 2 shows the values of [-?´(?, 0, ?)] for different values of ? and ?.

Huang and Chen [22] studied the effects of surface suction or blowing in a case of a cylinder subject to uniform heat flux density. Two models were used: two-temperature model and one-temperature model. Kimura [23] studied the transient problem and showed that the transient heat transfer for both forced and natural convection can be expressed in a unified manner with a single parameter representing the curvature effect of the cylinder surface. Yucel and Lai et al. [24, 25] studied combined heat and mass transfer problems in vertical cylinders. The mixed convection along a slender cylinder with variable surface heat flux considering Darcian flow problems were studied by Pop et al. [26]. This study also analyzed the effects of surface curvature and buoyancy in surface heat flux. The numerical solution of the transformed equations was obtained using the Keller box method to study the significant influence of these factors on the flow and heat transfer characteristics. The mixed convection along a cylinder with variable surface heat flux was analyzed by Aldoss et al [27]. When non-Darcy model was applied and nonsimilarity solutions were obtained for the case of variable wall temperature.

Table 2: Values of -?‵(0) for various values of ?‵for constant wall temperature ?=0 for the vertical cylinder case (Cheng and Minkowycz [21])

?—	-?´(0) at ?=0
0.25	0.4855
0.50	0.5272
0.75	0.5664
1.00	0.6049
2.00	0.7517
3.00	0.8915
4.00	1.024
5.00	1.154
6.00	1.283
7.00	1.413
8.00	1.544
9.00	1.678
10.00	1.815

Kumari and Nath [28] and Aldoss [29] analyzed the mixed convection problem for conduction fluids under magnetic fluid.

1.2.4. Natural Convection from Embedded Horizontal Cylinders

Merkin [30] studied the problem of a horizontal cylinder embedded in porous media. This is a special case of a general two-dimensional heated object that he analyzed. For the large Rayleigh number, the heat transfer coefficient can by calculated using:

$$Nu = 0.565\, Ra^*_D{}^{1/2} \tag{20}$$

where;

$$Nu = \frac{\bar{h}D}{k}$$

$$Ra^*_D = \frac{gdK(T_w - T_\infty)}{\alpha_m}$$

α_m = Thermal diffusivity for porous media

$\bar{h}$ = average heat transfer coefficient

The results were later generalized by Chen and Chen [31] for fluids with non-Newtonian viscosities. They extended it to power law fluids. Fand et al. [32] studied heat transfer problems and conducted experiments in porous media packed with random glass spheres using different fluids. This study suggested the following relationships for different ranges of Reynolds numbers:

For 0.001 < Re_{max} =ã3

$$Nu\,Pr^{0.0877} = 0.618 Ra^*_D{}^{0.698} + 8.54\times 10^6\, Ge\, Sech(Ra^*_D) \quad \text{for} \quad 0.001 < Re_{max} \le 3 \tag{21}$$

$$\mathrm{Nu\,Pr}^{0.0877} = 0.766\mathrm{Ra}^{*\,0.37}_{D}\left(\frac{C_1 D}{C_2}\right)^{0.173} \quad \text{for} \quad 3 < \mathrm{Re}_{max} \leq 100 \qquad (22)$$

where,

$$\mathrm{Nu} = \frac{\bar{h}\,D}{k}$$

$$\mathrm{Ge} = \frac{g\ D}{C_p}$$

C_1 and C_2 are constants.

The problem of horizontal cylinders embedded in a semi-infinite porous media was analyzed by Farouk and Shayer [33]. The heat transfer experiments of this problem were done by Fernandez and Schrock [34]. Cheng [34] studied the problem of mixed convection about a horizontal cylinder. Others, like Sano [36], Ingham et al. [37], Pop et al. [38, 39], Tyvand [40], Sundfor and Tyvand [41] and Bradean et al. [42] used detailed analytical and numerical analysis of transient natural convection from embedded horizontal cylinders.

1.2.5. Natural Convection from Embedded Vertical Cones

Considerable analytical and numerical works are available in the literature due to the importance of cone and conical frustum embedded in porous media in many applications. Cheng et al. [43] analyzed the problem of conical frustum with a power law temperature or a power law heat flux at the surface. Results can be summarized as follows for constant wall temperature:

$$\mathrm{Nu_x} = 0.769\mathrm{Ra}{*}_x^{1/2} \qquad (23)$$

where, $\mathrm{Ra_x} = \dfrac{g \;\; \mathrm{K}\cos(\gamma)(\mathrm{T_w} - \mathrm{T_\infty})x}{\alpha_m}$,

and x = distance from apex along the surface.

For constant wall heat flux:

$$Nu_x = \frac{\hat{\mathrm{Ra}}^{1/3}}{1.056} \qquad (24)$$

where, $\hat{\mathrm{Ra}} = \dfrac{g \;\; \mathrm{K.}\cos(\gamma) q_w^{"} \mathrm{x}^2}{\alpha_m \mathrm{k_m}}$

Pop and Cheng [44] included the curvature effect. Corresponding non-Darcian problems were addressed by Vasantha et al. [45], Nakayama et al. [46]. The problem of combined heat and mass transfer was analyzed in porous media saturated with Newtonian fluids by Yih [47, 48, 49] and with non-Newtonian fluids by Yih [50] and Yang and Wang [51]. Triphathi et al. [52] and Ramanaiah and Malarvizhi [53] included the effect of thermal stratification of the porous media. Heat and mass transfer was also analyzed by Rahman and Faghri [54, 55, 56]. Hydro-magnetic effect of the conducting fluid starting the porous media has been included by Kafoussias [57] and Chamkha [58]. Natural convection form a frustum of a wavy cone embedded in saturated porous media was analyzed by Pop and Na [59].

CHAPTER 2

DESCRIPTION OF THE PROBLEM

From the presented literature review it is evident that there are no experimental data available on natural mass/heat transfer from vertical cylindrical surfaces embedded in saturated porous media. These data are essential to validate/discriminate different theoretical studies and to analyze several engineering application. In this work, the mass transfer coefficients for vertical cylinders are obtained using limiting diffusion current technique. This technique utilizes cupric ion reduction on the vertical cylindrical surfaces, which are embedded in the desired porous medium.

CHAPTER 3

EXPERIMENTAL SET-UP AND PROCEDURE

3.1. Preparation of Copper Electrodes and Porous Media

Cylindrical copper electrodes of a wide range of sizes were prepared to cover a considerable range of Rayleigh number. The bigger cylinders were fabricated from commercial copper tubes while for the smaller diameter copper wires were used. The bigger cylinders were welded with copper wire for electrical connections. Ends of the tubes were carefully sealed. For smaller diameter cylinders, a copper wire was stretched in a specially designed holder as shown in Figure 1. The surfaces of these cylinders were masked with an insulating paint such as to provide desired mass transfer area. Diameter and length of the cylinders were varied as shown in Table 3. The porous media were prepared using packing material of glass spheres of diameters 2, 3, 4, 6 mm.

Figure 1: Holder for small diameter cylinders.

Table 3: Diameter and length of copper cylinders used in this work

Sample	**Diameter (mm)**	**Length(cm)**
Cylinder 1	0.65	1.0, 2.0, 3.0, 4.0, 5.0, 6.0, 7.0
Cylinder 2	0.10	1.0, 2.0, 3.0, 4.0, 5.0, 6.0, 7.0
Cylinder 3	3.16	1.0, 2.0, 3.0, 4.0, 5.0, 6.0, 7.0
Cylinder 4	9.00	1.0, 2.0, 3.0, 4.0, 5.0, 6.0, 7.0
Cylinder 5	13.00	1.0, 2.0, 3.0, 4.0, 5.0, 6.0, 7.0
Cylinder 6	22.00	1.0, 2.0, 3.0, 4.0, 5.0, 6.0, 7.0
Cylinder 7	28.00	1.0, 2.0, 3.0, 4.0, 5.0, 6.0, 7.0

3.2. The Experimental Setup

The experimental set-up used in this study is illustrated in Figure 2. The copper surface, on which the mass transfer coefficient is to be determined, functions as working electrode in the electrochemical cell. The working electrode was embedded in a bed of various porous material made of glass spheres. A copper cylinder kept inside the bed near to the wall acts as the counter electrode. A saturated calomel electrode functions as the reference electrode and was embedded in the porous media. Copper reduction from acidic cupric sulfate solution was used to estimate mass transfer coefficients for the advantages mentioned earlier.

The porous media was formed using different glass packing material in a one liter cylindrical beaker. A solution 0.0529 M $CuSO_4$ and 3.03 M H_2SO_4 was prepared. Concentrations of Cu^{++} and H_2SO_4 were determined through idiometric and acid-base titration procedures. Porosities of the packing material were determined by water replacement method, where the amount of water necessary to fill the void between the glasses spheres was measured.

The copper surfaces were cleaned using emery papers of different sizes (100, 400, 600 and finally 1500 grit sizes). Subsequently, they were cleaned with acetone to remove any grease or oil. If any surface is to be insulated, an insulating paint was used.

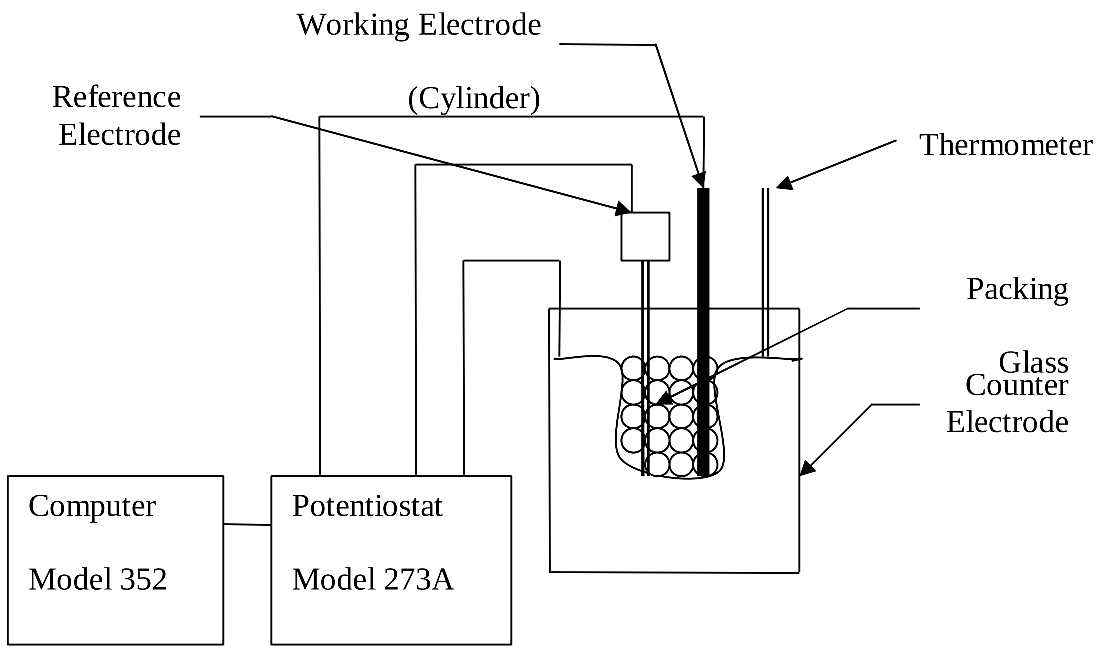

Figure 2: Experimental Set-up Illustration

The temperature of the solution was measured and recorded using a thermometer of 0.1 °C least count. The working electrode, counter electrode and the reference electrode were connected to a potentionstat (Model 273A, EG&G PARC). The potentiostat was driven by a manufacturer software package (Model 352, EG&G PARC) via a microcomputer. Linear polarization curves were obtained for all samples in all packing materials (Appendix A). The electrochemical parameters maintained during the experiments are listed in Table 4. Figure 3 and Figure 4 show the photographs of the experimental set-up and the electrochemical cell.

Table 4: Parameters of linear polarization experiments.

Parameter	Value	Unit
Conditioning Time	60	seconds
Initial Potential	-50.00	mV SCE
Conditioning Potential	-100.00	mV SCE
Final Potential	-850.0	mV SCE
Scan Rate	1.500	mV/s
Scan Increase	1.000	mV
Step Time	666.7×10^{-3}	VHFRQG
Reference Electrode	241.5	mV SCE
Sample Area	1.000	cm^2

Figure 3: Photograph of the experimental setup

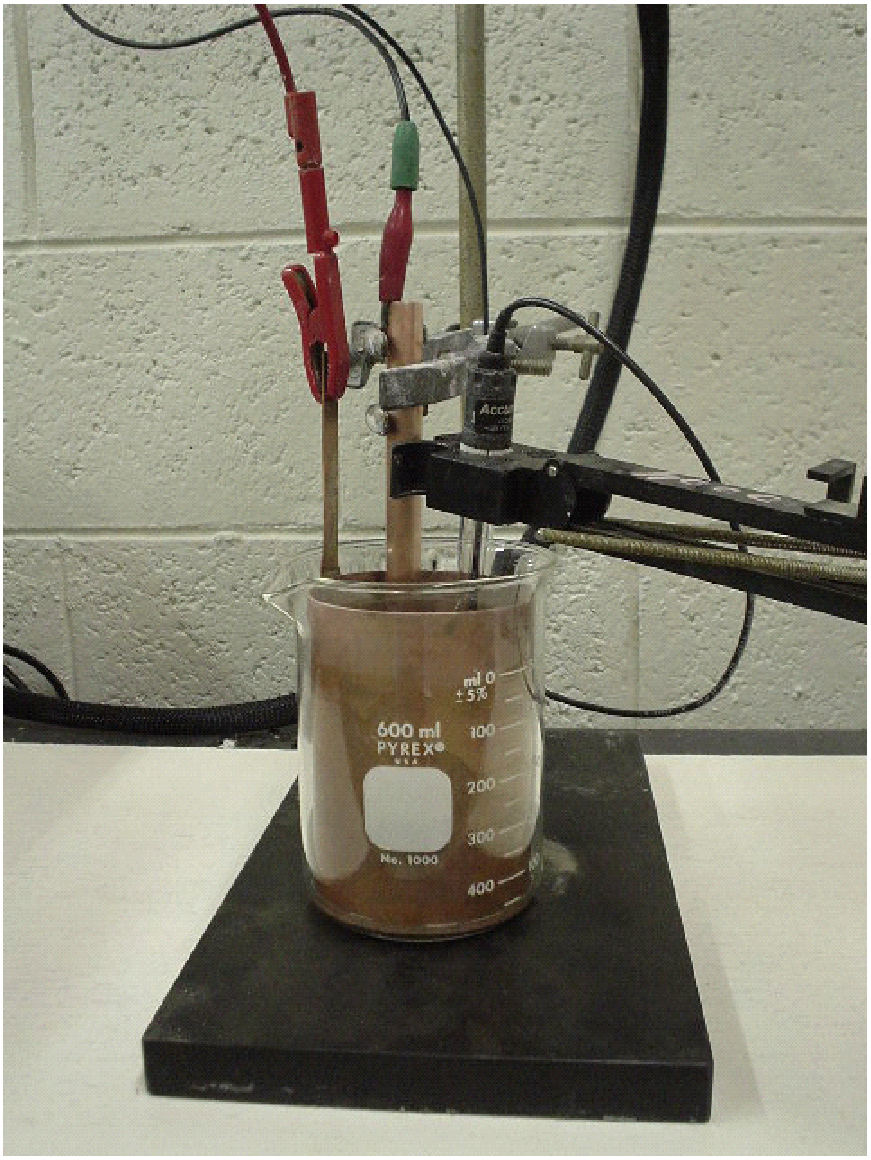

Figure 4: Electrochemical cell for measurement of the limiting current

3.3. Data Reduction

3.3.1. Physicochemical Properties of Electrolyte

It is necessary to use accurate data for of the physicochemical properties of the electrolyte solution. The density, viscosity and diffusivity of Cu^{++} are necessary in calculating the mass transfer coefficient. The following correlations are used to estimate the properties of acidic cupric sulfate solution [20]:

$$(gm/cm^3) = 0.999448 + 0.14807C_b + 0.060816C_{Acid} - 4.246\times10^{-4}\Delta T + 0.00151(C_b)^2 - 7.043\times10^{-4}(C_{Acid})^2 - 4.47\times10^{-6}\Delta T^2 - 0.00456C_bC_{Acid} - 6.0\times10^{-5}C_b\Delta T + 1.81\times10^{-5}C_{Acid}\Delta T \quad (25)$$

$$\mu(poise) = 0.01\times[0.89954 + 0.4537C_b + 0.14063C_{Acid} - 0.019235\Delta\mathrm{T} + 0.232(C_b)^2 + 0.02894(C_{Acid})^2 + 0.000321\Delta\mathrm{T}^2 + 0.09496C_bC_{Acid} - 0.0154C_b\Delta\mathrm{T} - 0.004953C_{Acid}\Delta\mathrm{T}] \quad (26)$$

$$\mathrm{D}_{\mathrm{Cu}++}(\mathrm{cm}^2/\mathrm{s}) = ((\mathrm{T} + 273.15)/\mu)\times 2.09\times10^{-10} \qquad (\text{when } C_b < 0.09\text{ M})$$

(27)

$$\mathrm{D}_{\mathrm{Cu}++}(cm^2/s) = ((\mathrm{T} + 273.15)/\mu)(1.98 + 2.34C_b)\times10^{-10} \quad (\text{when } C_b \geq 0.09\text{M})$$

Where,

?ëT = (T-25) °C

C_b = bulk concentration of copper sulfate (mol/liter)

C_{Acid} = bulk concentration of acid (mol/liter)

μ#= Viscosity (poise)

3.3.2. Determining Sherwood and Rayleigh Numbers

The mass transfer coefficient calculated by Equation (2) was used in the calculation of the Sherwood number:

$$Sh_L = k_L L/D \quad \text{and } Sh_L^* = k_L L/D_e \qquad (28)$$

where, D_e=D*ex/tx* and K = d_p^2*e*ã180(1-*e*)^2. The average modified Rayleigh number is calculated using the following relationships:

$$Ra_L = gL^3(?½?½ - 1)/\ \ D \text{ and } Ra_L^* = gKL(?½?½ - 1)/\ \ D_e \qquad (29)$$

Where density at the surface is denoted by ?$_0$Á and is calculated using the relationship given in previous section, substituting a value of zero for the concentration of C_b of $CuSO_4$. The concentration of H_2SO_4 at the surface can be estimated using the following relationship [6]:

$$C_{Acid,\,s} = C_{Acid,\,b} - \left[\frac{D_{cu^{++}}}{D_{H^{++}}}\right]^{1-n}\left[\frac{t_{H^{++}}}{1-t_{cu^{++}}}\right]C_b \qquad (30)$$

where,

$$t_{Cu^{II}} = \left(0.2633 - 0.1020C_{Acid,b}\right)C_b$$

$$t_{H^+} = 0.8156 - 0.2599C_b - 0.1089C_b^2$$

$$D_{H^+}(cm^2/s) = ((T + 273.15)/\mu)(5.655 + 3.274C_b + 0.831C_{Acid,b}) \times 10^{-10}$$

CHAPTER 5

RESULTS AND DISCUSSION

5.1. Polarization Curves

The linear polarization curves obtained for all cylinders in free solution and in saturated porous media are compiled in Appendix A. Figure 5a shows a typical polarization curve. The polarization curves exhibit three regions. In the first region, the current increases with increasing potential. In this region the overall reaction is controlled by both mass transfer and electrochemical reaction. In the second region, the current becomes almost constant that manifests itself as a plateau in the polarization curve. The over all rate of reaction is determined by mass transfer only. The current corresponding to the plateau is called the limiting current and is recorded. In the third region, the current increases sharply associated with lots of gas bubbling on the electrode surface. This is due to the hydrolysis of water. The current in this region corresponds to the overall rate of reaction for hydrolysis of water.

In Figure 5b, a sharp increase is noticed in the current in the beginning. The experiment starts with -50.00E-3 V SCE which makes the working electrode an anode. Therefore, in the beginning of the experiment slight anodic dissolution of the electrode takes place. It increases local copper ion concentration. As the potential increases, the electrode becomes a cathode and deposition of copper ions starts to take place. Since the local concentration of copper ions was high, the polarization curve shows a sharp increase in the current as soon as the potential becomes cathodic.

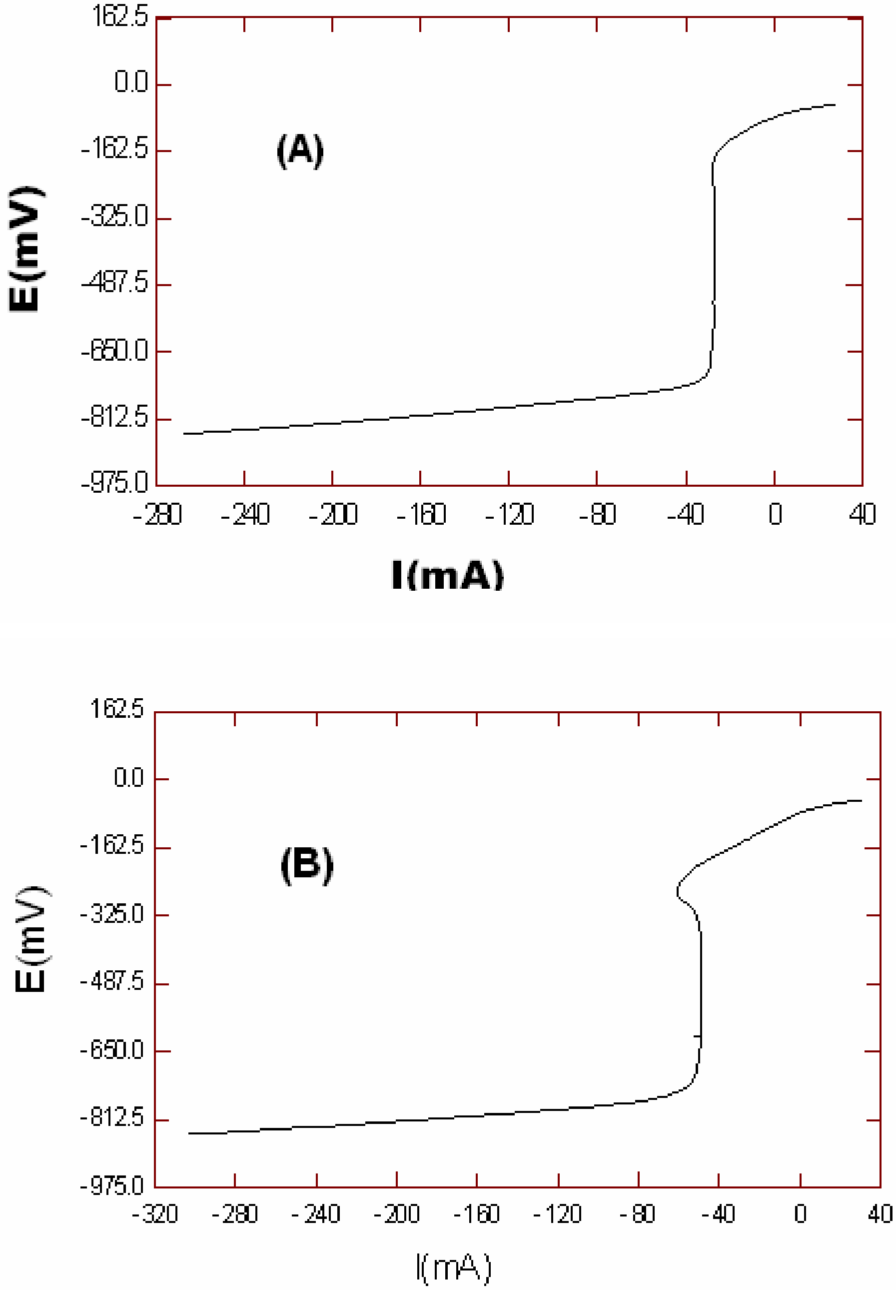

Figure 5: Typical polarization curve for cylinders in free solution

Once all the dissolved ions are deposited, the current returns to its value that correspond to the bulk copper ion concentration.

5.2. Natural Convection on Vertical Cylinders of Various Aspect Ratios in Free Solution

The average mass transfer coefficients estimated by Equation (2) are plotted against embedded lengths for free solution in Figure 6 through Figure 12. The mass transfer coefficients decrease with increasing length, conforming to the inferences of the boundary-layer theory. The mass transfer coefficient is the highest in the case of free solution because of the low resistance to the rate of transfer. The data were acquired at room temperature which remained almost constant during an experiment but varied between different experiments. The temperatures were recorded accurately for each experiment. Since the physico-chemical properties of the solution are strong functions of temperature, the measured mass transfer coefficients have significant influence of randomly varying temperature. Therefore the dependency of the mass transfer coefficient on packing material cannot be established on the basis of k_L vs. x curves without non-dimensionalization.

Average Sherwood number Sh_L is plotted against Ra_L for various cylinders in Figure 13. The data exhibit power law relationship indicated by straight lines on logarithmic plots. For larger cylinders, all data seem to fall on one single line corresponding to the vertical

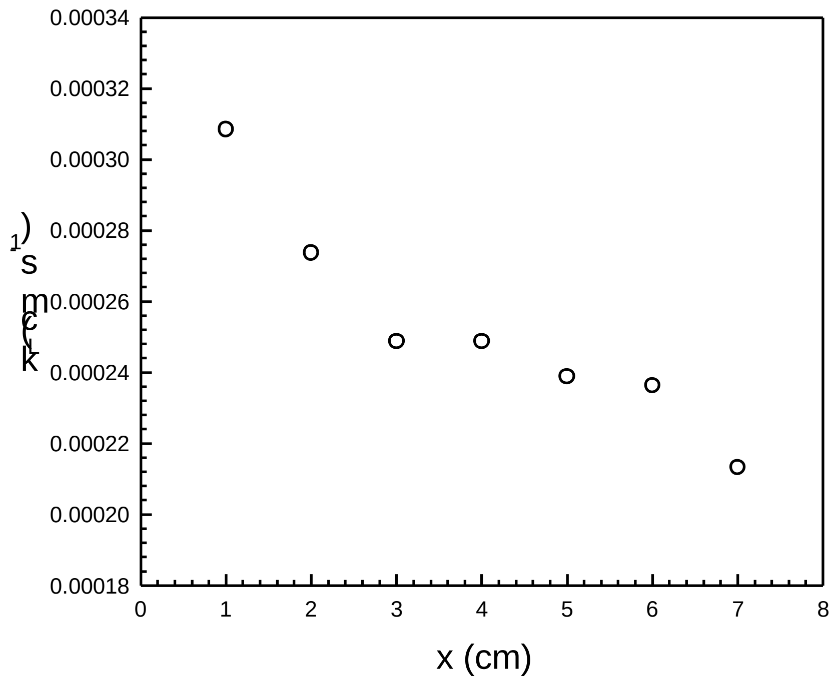

Figure 6: Mass transfer coefficient vs. vertical distance for Cylinder 1 in free solution

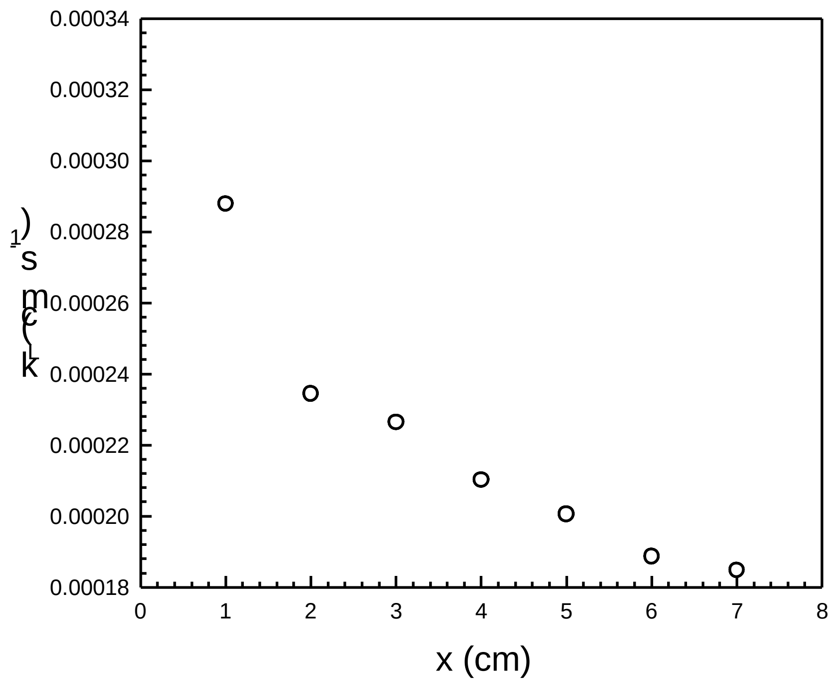

Figure 7: Mass transfer coefficient vs. vertical distance for Cylinder 2 in free solution

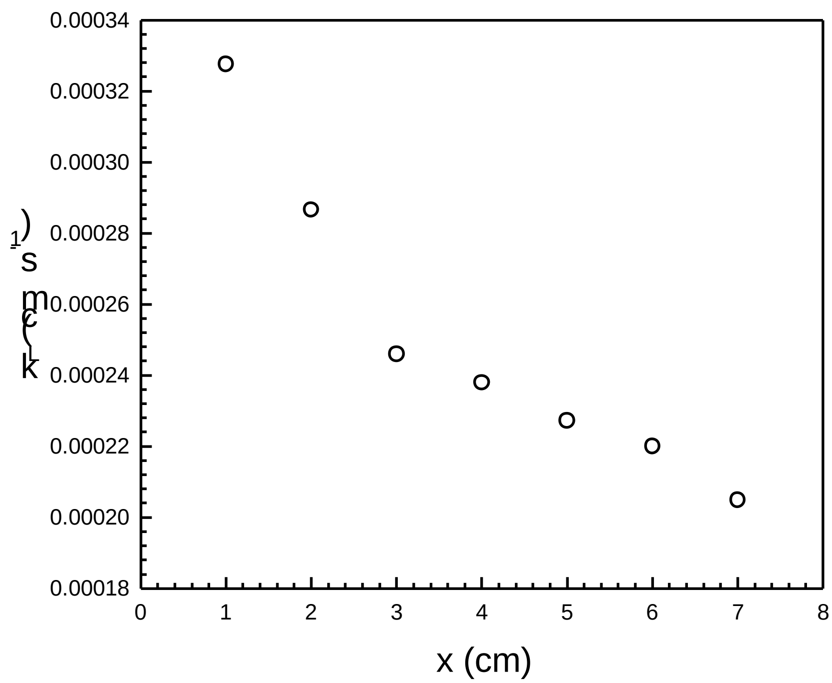

Figure 8: Mass transfer coefficient vs. vertical distance for Cylinder 3 in free solution

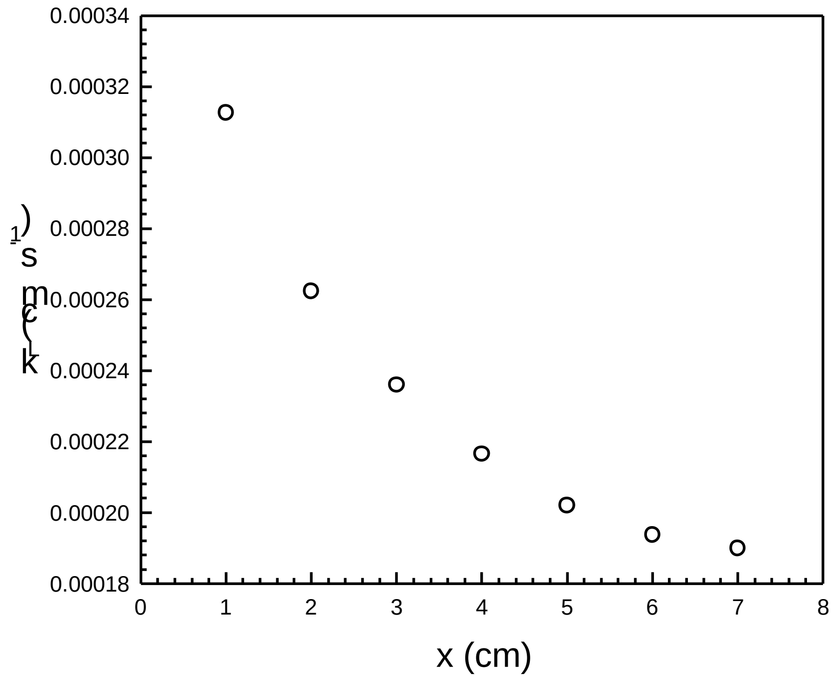

Figure 9: Mass transfer coefficient vs. vertical distance for Cylinder 4 in free solution

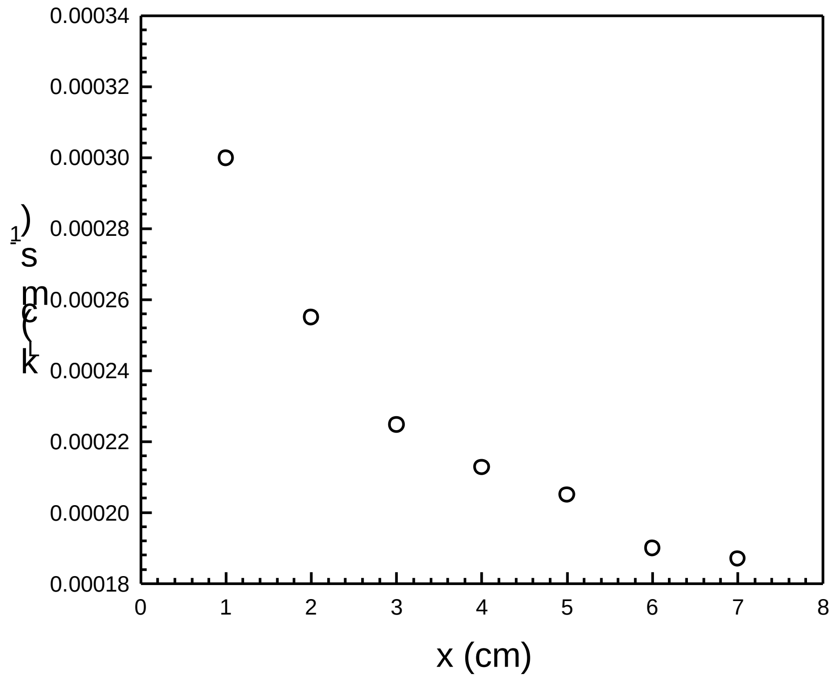

Figure 10: Mass transfer coefficient vs. vertical distance for Cylinder 5 in free solution

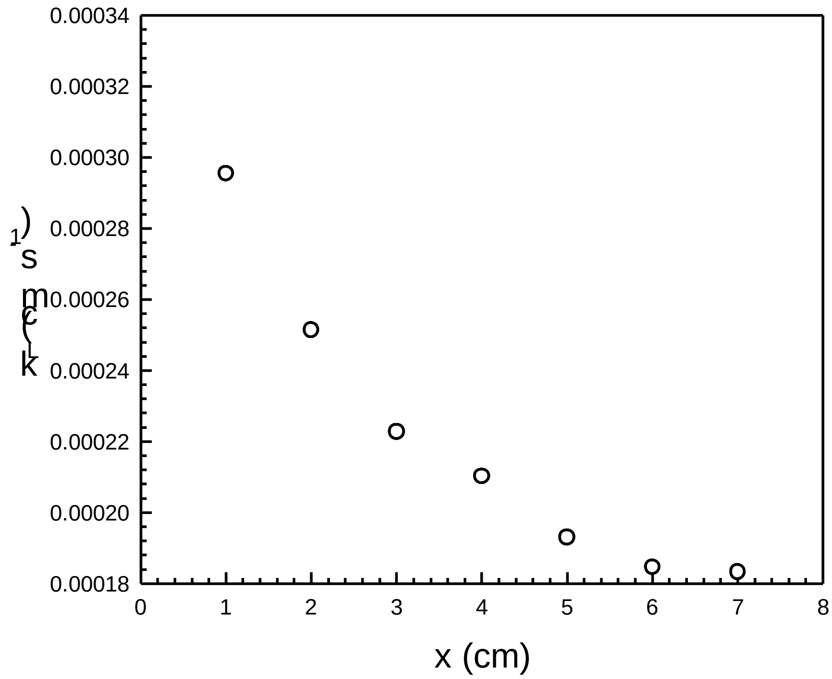

Figure 11: Mass transfer coefficient vs. vertical distance for Cylinder 6 in free solution

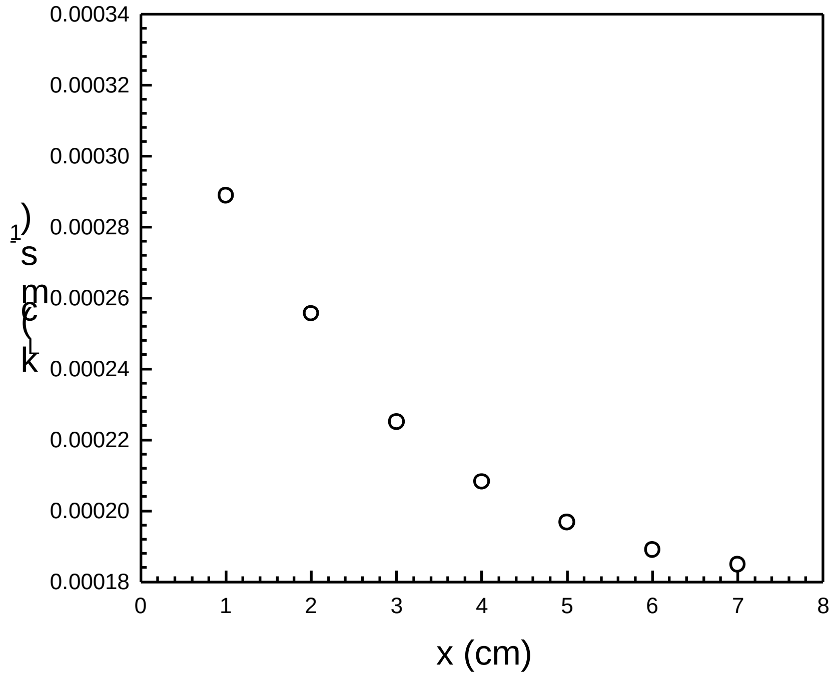

Figure 12: Mass transfer coefficient vs. vertical distance for Cylinder 7 in free solution

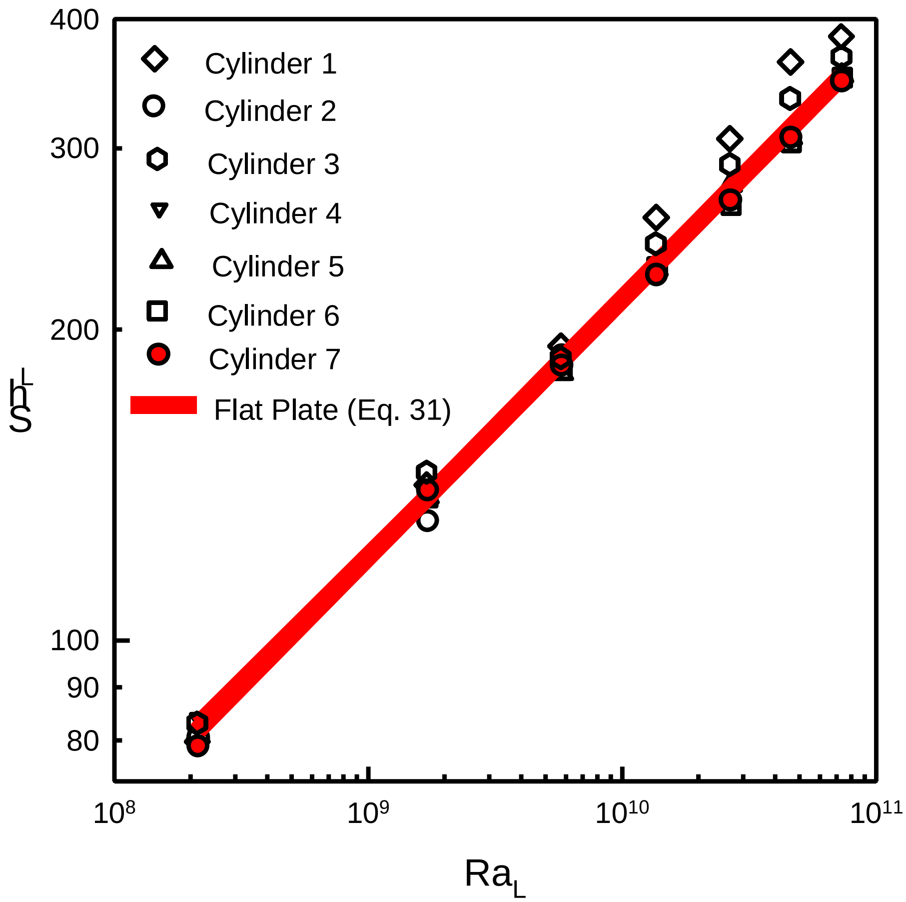

Figure 13: Average Sherwood Number vs. Rayleigh Numbers for Different Cylinders in Free Solution

flat plate, for which mathematical expression was developed using the boundary layer theory [60]:

$$Sh_L = 0.677\,Ra_L^{0.25}\left[\frac{0.952}{Sc}+1\right]^{-.025} \tag{31}$$

where Sc = *v*/D

The Sherwood numbers for smaller diameter cylinders are relatively higher. In other words, the effect of the curvature is perceptible only for very small cylinders (Cylinder 1, Cylinder 2 and Cylinder 3). Ravoo et al [61] studied the effect of the curvature on the transport process. Corresponding mass transfer equation is given by:

?ó=3/80aô^4+16/225 aô^5+19/252 aô^6+17/294 aô^7+ . . . . . . (32)

where, ?9= x/RRa$_L^{1/4}$, which is a dimensionless curvature parameter, and 1/ a9= Sh$_{r\text{-}L}$, where, Sh$_{r\text{-}L}$ = k$_L$R/D, which is a Sherwood number based on the radius of the cylinder.

Equation (32) exhibits a straight line behavior at small values of curvature parameter (?). At these low values, the mass transfer for cylinders can be approximated to that of flat plate. The effect of curvature becomes significant at higher values of ?,™influenced by high value of aspect ratio. Figure 14 shows the experimental data in agreement with the model at low values of ?Lwhere the data are in close agreement with flat surfaces. As ?L exceeds 0.1, the effect of curvature becomes significant and the flat surfaces approximation is not valid. The experimental data are in agreement with Equation (32), however it underpredicts Sh$_{r\text{-}L}$ for very small diameters.

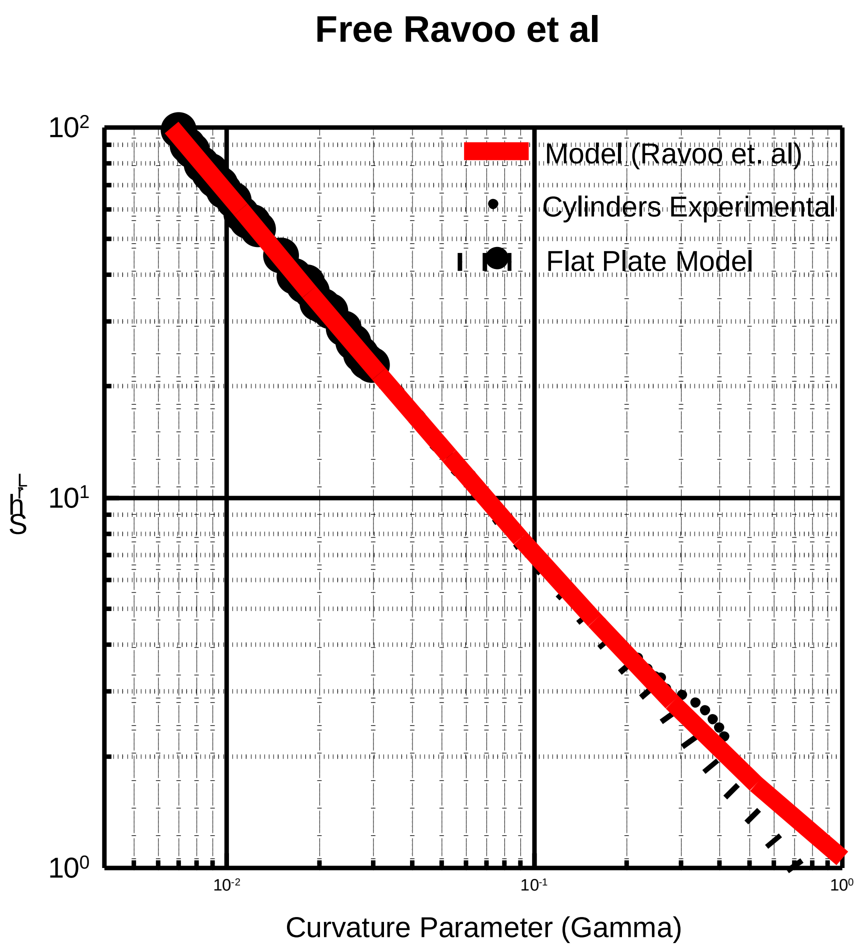

Figure 14: Average Sherwood Number vs. curvature parameter for different Cylinders in free solution.

5.3. Natural Convection on Vertical Cylinders of Various Aspect Ratios in Saturated Packed Media

Polarization experiments were performed for seven different vertical lengths of six different cylinders embedded in porous media made of glass spheres of 6 mm, 4 mm, 3 mm and 2 mm diameters. The polarization curves for each data-point in a representative run are given in Appendix A.

The average mass transfer coefficients estimated by Equation (2) are plotted against the vertical distance from the leading edge (x) in various packing media sizes in Figure 15 through Figure 20. Similar to the case of natural convection in free solution, the mass transfer coefficients decrease with increasing length, conforming to the boundary-layer theory. In general, the mass transfer coefficient increases with the particle size of the packing, approaching the values for the free solution as shown. Because the temperature varied between different experiments, the dependency of the mass transfer coefficient on packing material cannot be established on the basis of k_L vs. x curves without non-dimensionalization. Therefore, the average values of Sh_L and Ra_L were calculated.

Figure 21 through Figure 26 show Sh_L vs. Ra_L plots. In each of these figures values for all four packings have been plotted for one cylinder. Straight lines on the logarithmic scales indicate a power-law relationship between Sherwood number and Rayleigh number. Since the slope of the line does not change with Rayleigh number, it can be inferred that the flow was in the laminar regime for all data points. The value of

Sherwood number increases with size of the packing material, approaching towards those for the free solution.

The effect that curvature has on the mass transfer coefficients in porous media is shown in Figure 27 through Figure 30. In each of these figures, Sh_L is plotted against Ra_L for all six cylinders while embedded in one packing material. As expected, the mass transfer coefficients for smaller cylinders are higher. However, the effect of the curvature is perceptible only for very small cylinders (Cylinder 1 and Cylinder 2).

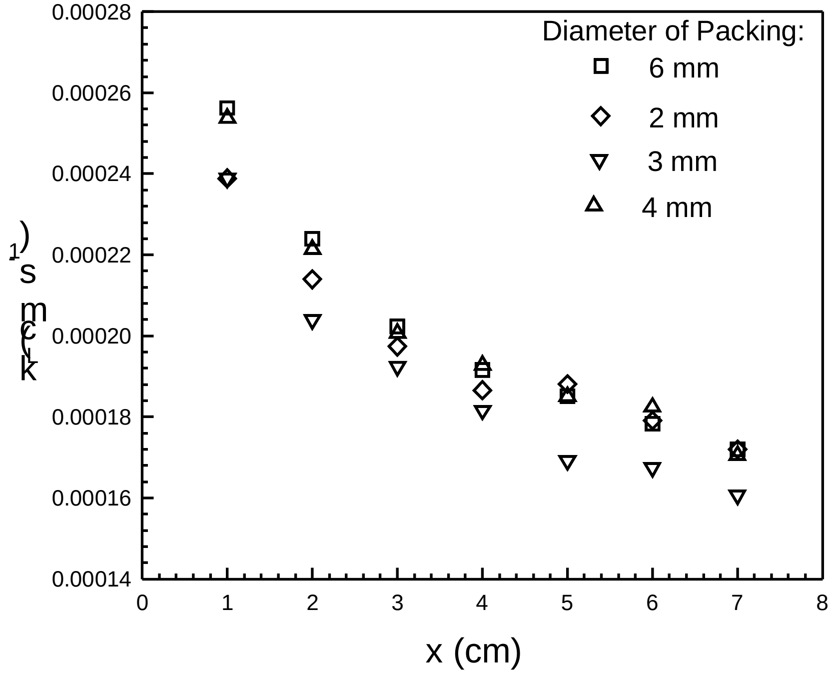

Figure 15 : Mass transfer coefficient vs. vertical distance for Cylinder 1 in porous media

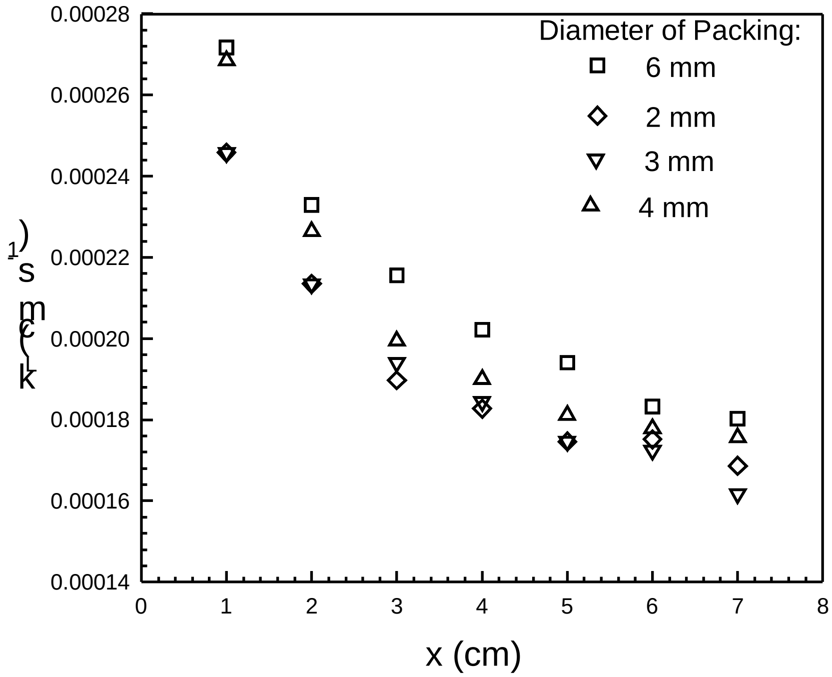

Figure 16: Mass transfer coefficient vs. vertical distance for Cylinder 2 in porous media

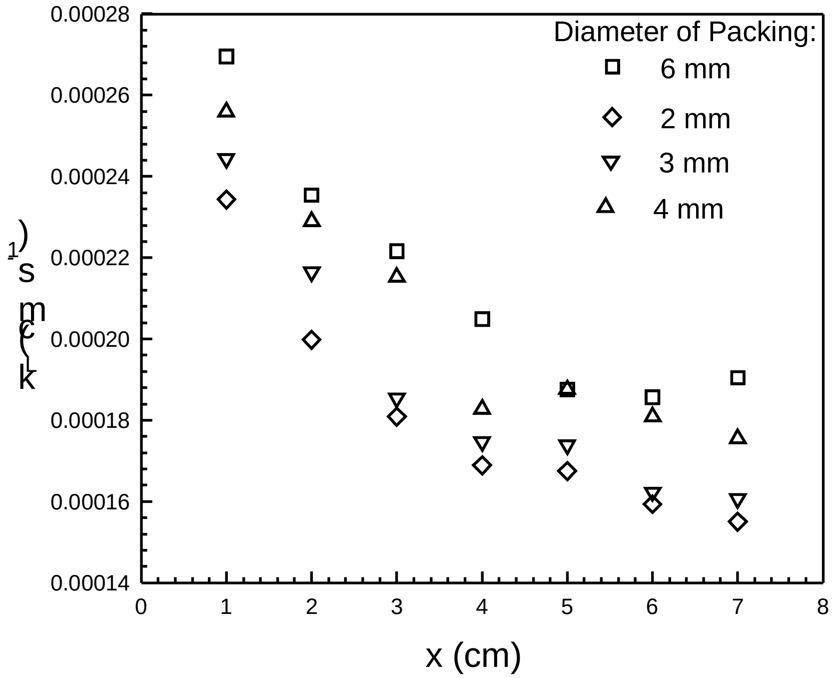

Figure 17: Mass transfer coefficient vs. vertical distance for Cylinder 4 in porous media

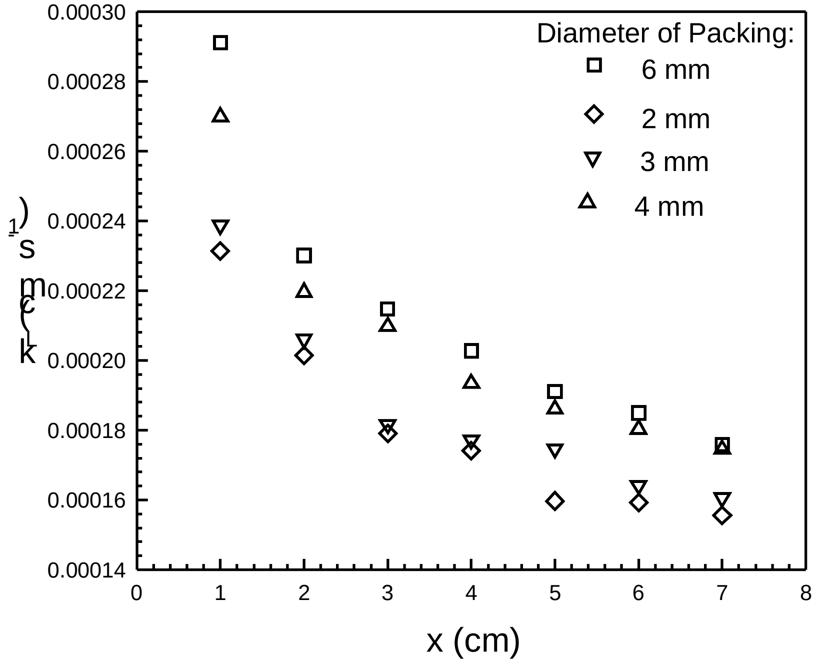

Figure 18: **Mass transfer coefficient vs. vertical distance for Cylinder 5 in porous media**

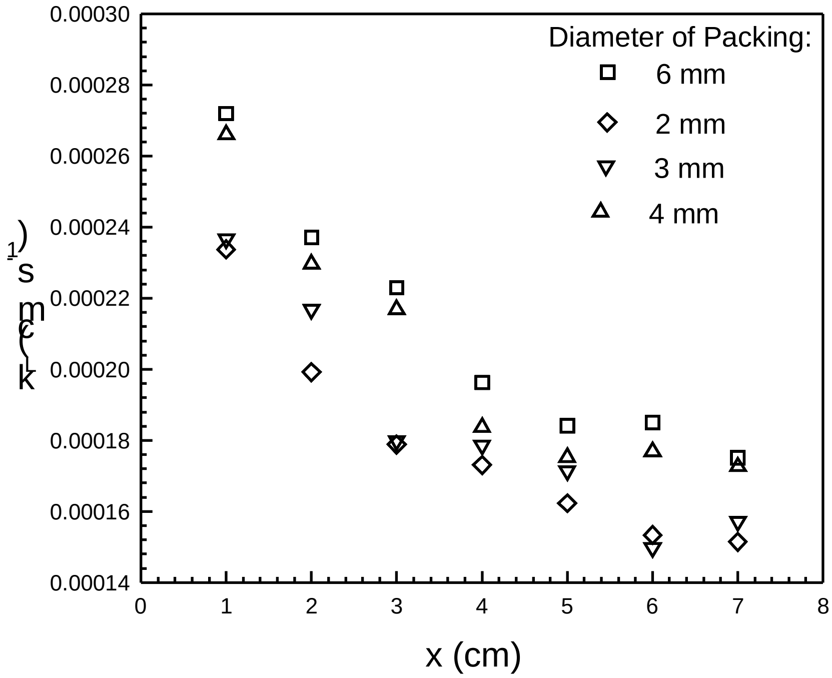

Figure 19: Mass transfer coefficient vs. vertical distance for Cylinder 6 in porous media

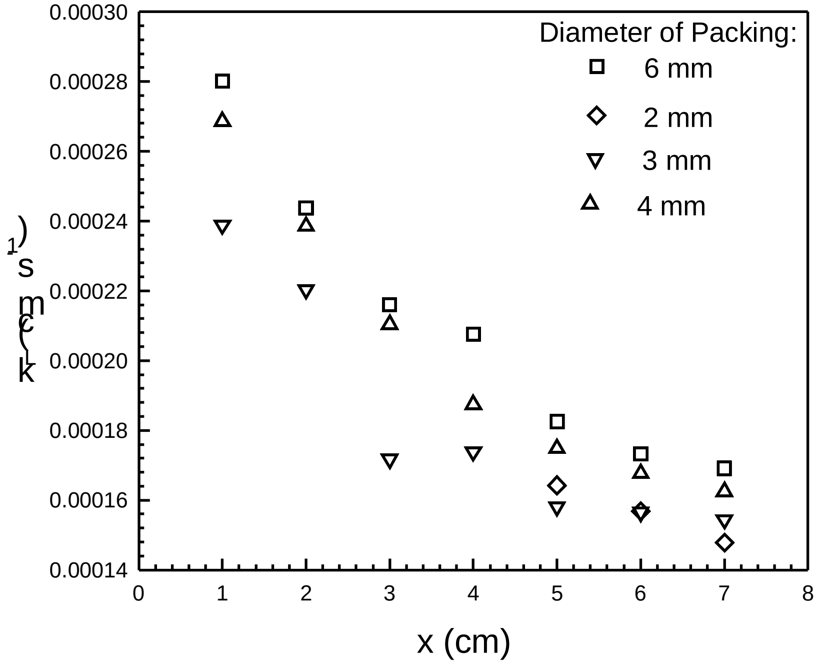

Figure 20: Mass transfer coefficient vs. vertical distance for Cylinder 7 in porous media

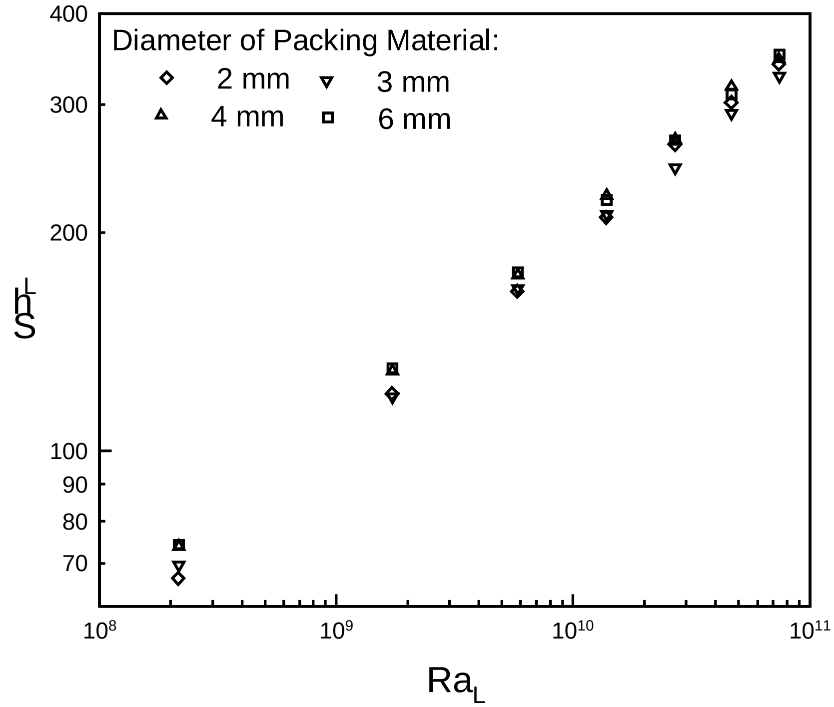

Figure 21: Average Sherwood number vs. Rayleigh number for Cylinder 1 in porous media

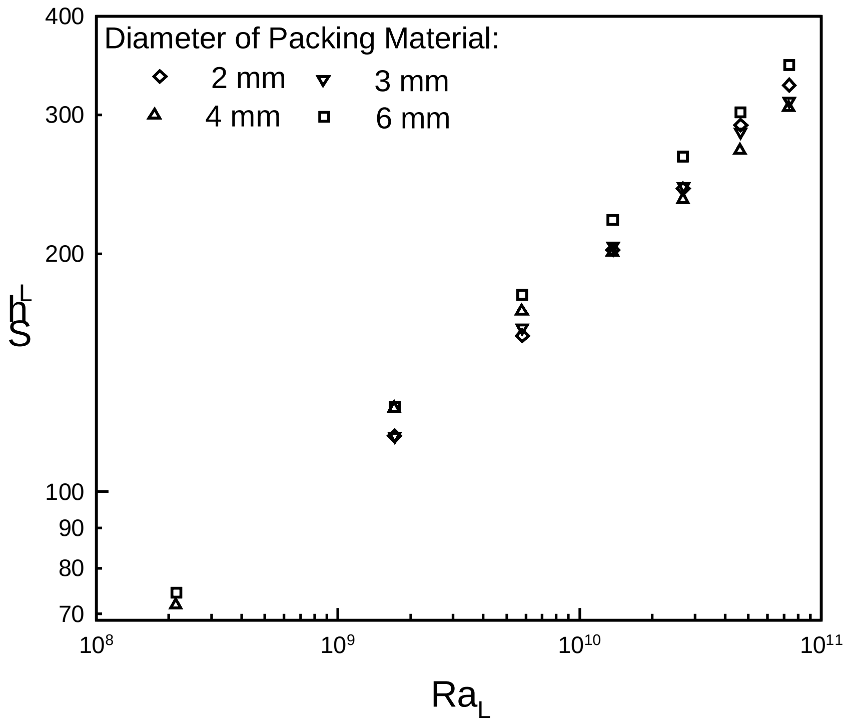

Figure 22: Average Sherwood number vs. Rayleigh number for Cylinder 2 in porous media

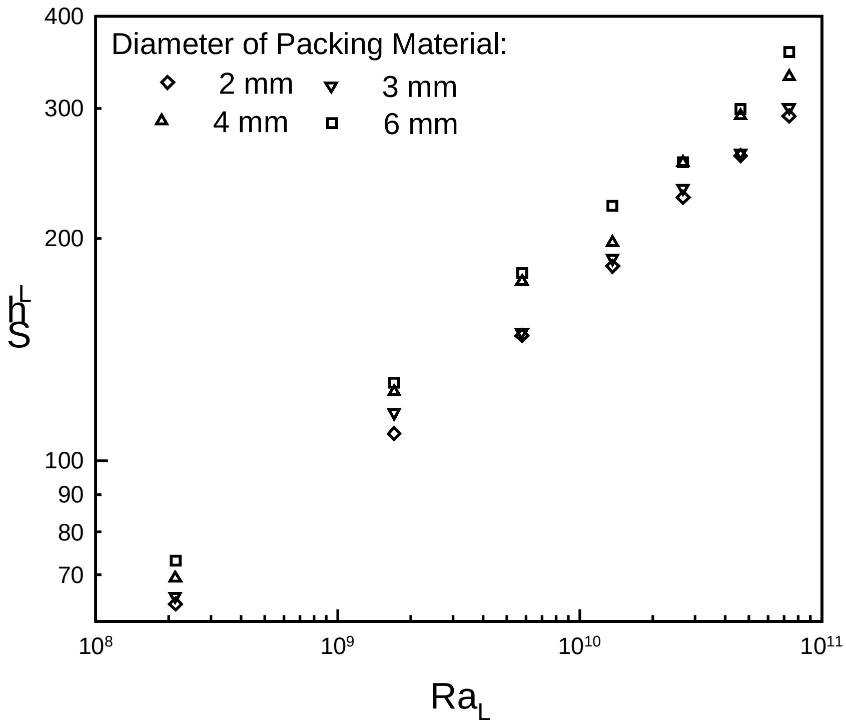

Figure 23: **Average Sherwood number vs. Rayleigh number for Cylinder 4 in porous media**

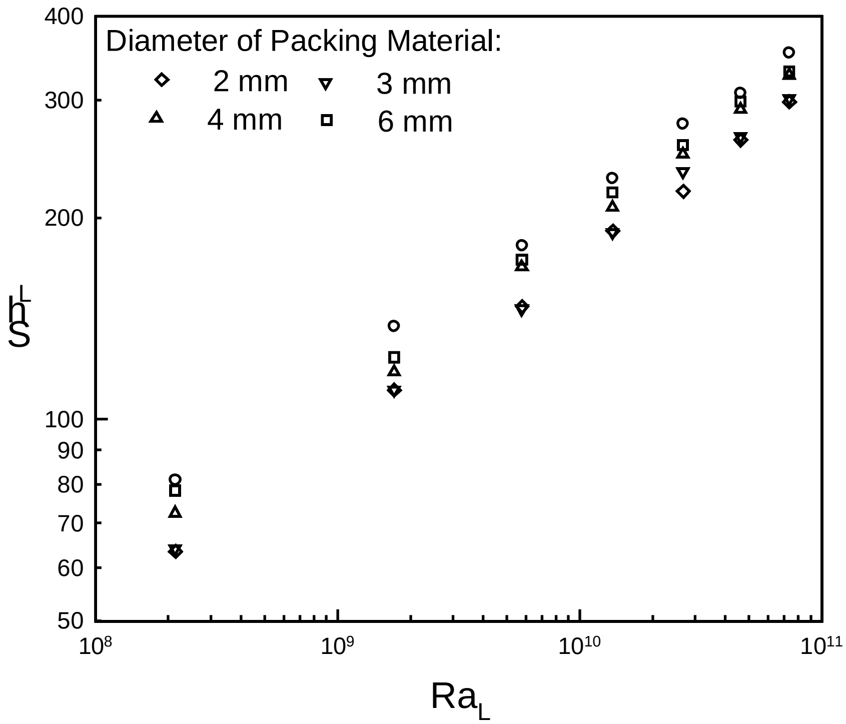

Figure 24: Average Sherwood number vs. Rayleigh number for Cylinder 5 in porous media

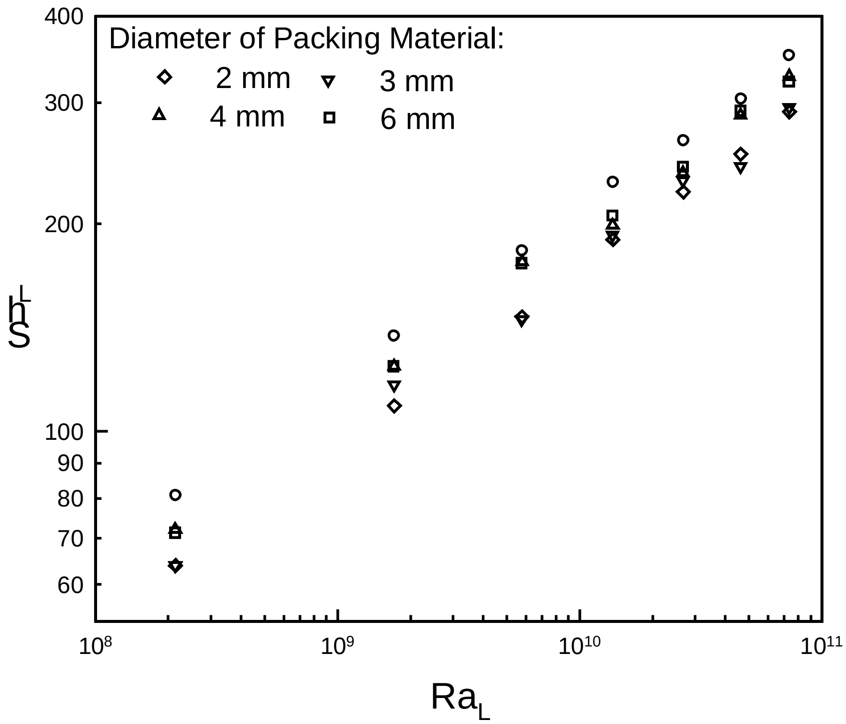

Figure 25: Average Sherwood number vs. Rayleigh number for Cylinder 6 in porous media

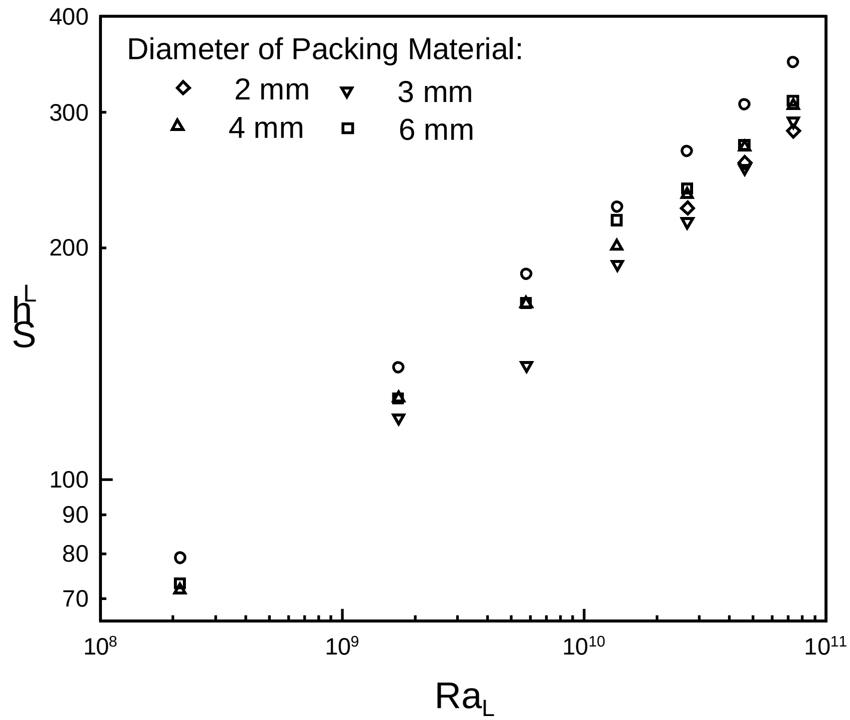

Figure 26: Average Sherwood number vs. Rayleigh number for Cylinder 7 in porous media

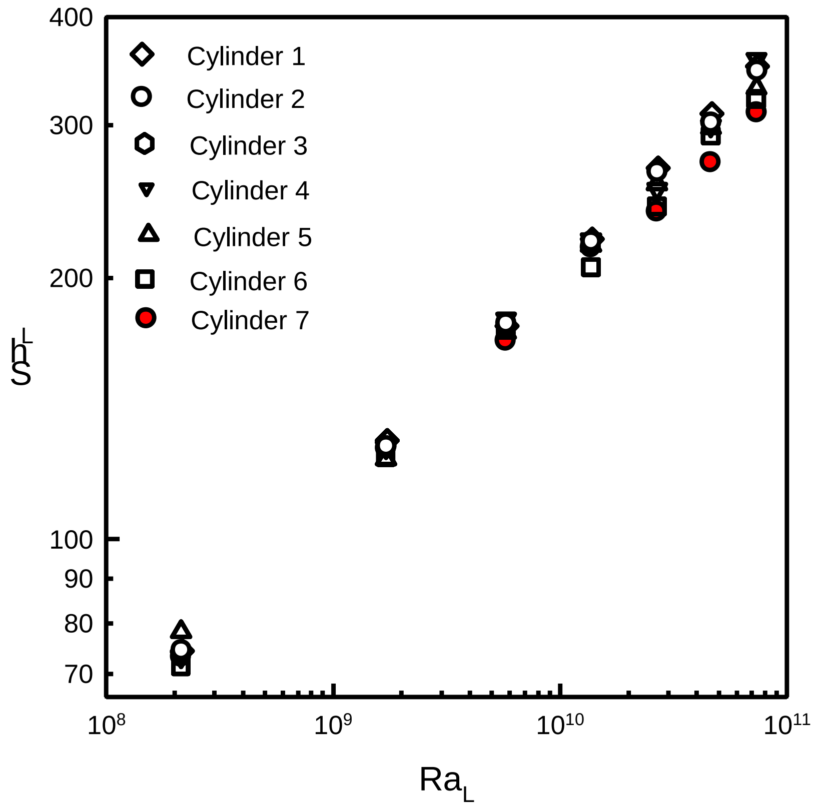

Figure 27: **Average Sherwood number vs. Rayleigh number for various cylinders in porous media of 6 mm glass spheres**

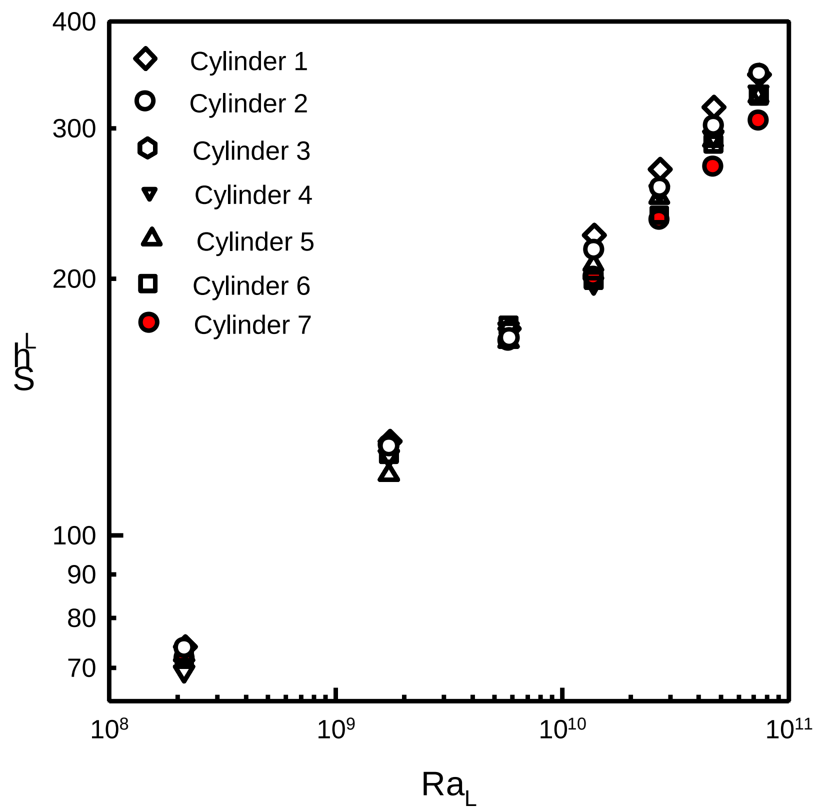

Figure 28: **Average Sherwood number vs. Rayleigh number for various cylinders in porous media of 4 mm glass spheres**

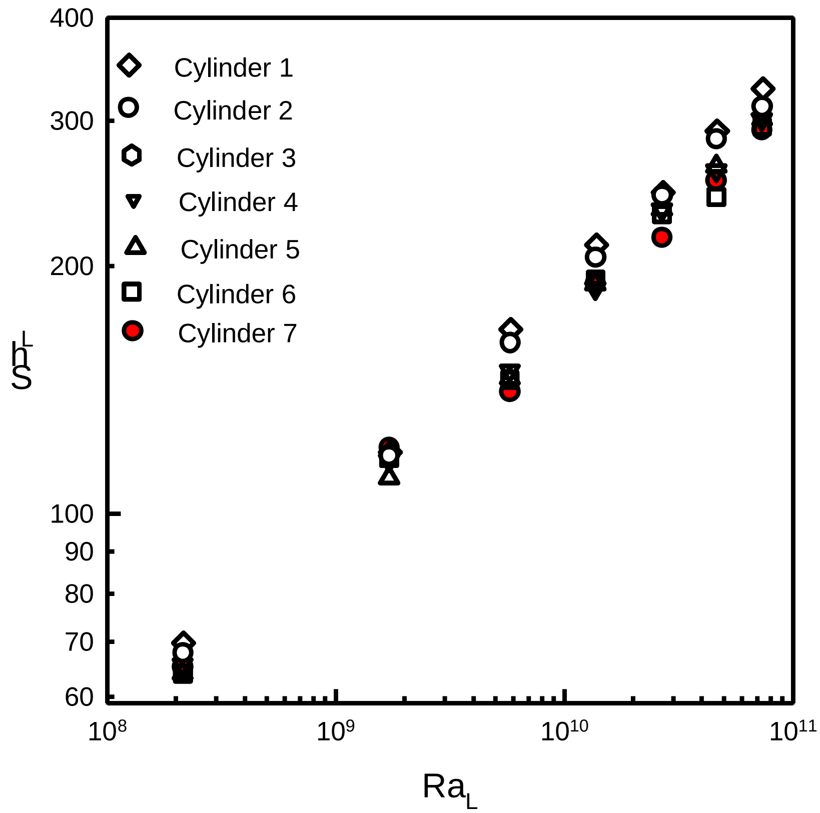

Figure 29: **Average Sherwood number vs. Rayleigh number for various cylinders in 3 mm glass spheres**

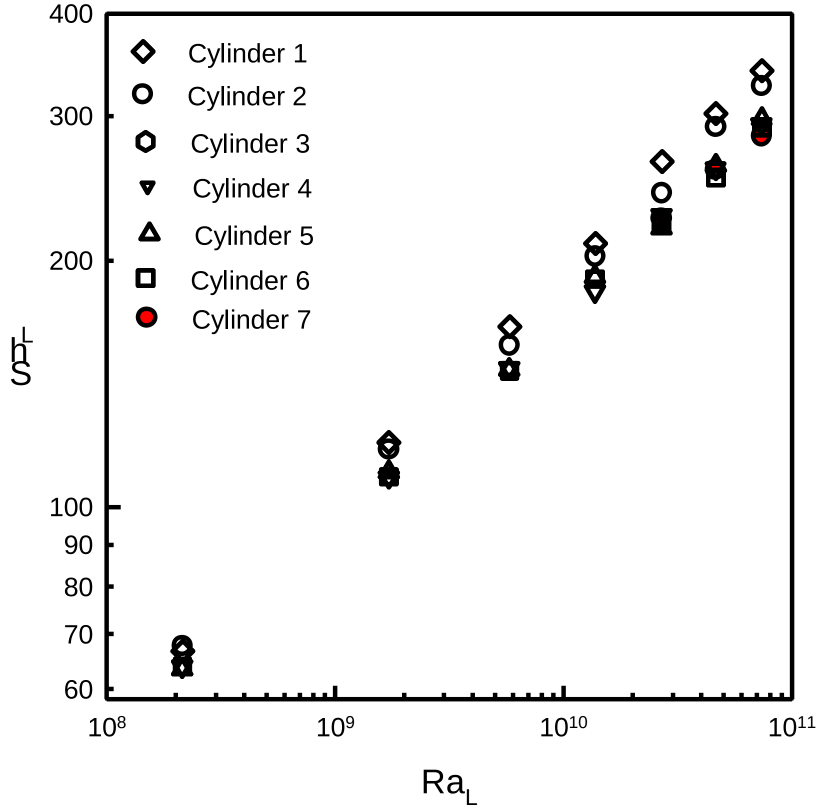

Figure 30: Average Sherwood number vs. Rayleigh number for various cylinders in porous media of 2 mm glass spheres

The modified average Sherwood number (Sh_L*) calculated using effective diffusivity is plotted against the modified Rayleigh number (Ra_L*) in Figure 31 through Figure 36 for each cylinder. The experimental data for different packing materials form straight lines of approximately the same slope. Sh_L* decreases with increasing particle size for a given Ra_L*. However, it is difficult to correlate all the data in one equation using these plots.

Kim and Vafai [16] used Brinkman-extended Darcy model to predict heat transfer coefficients from vertical flat plates embedded in porous media. They have shown that a relation between Sh_L* and. Ra_L*/Da_L exists. Rahman et al [20] have obtained experimental data using LDCT for vertical flat plates embedded in saturated porous media and proposed following correlation:

$$Sh_L^*(\text{Plate}) = 3.32\left(\frac{Ra_L^*}{Da_L}\right)^{0.26} \qquad (33)$$

Following these studies, the Sh_L* is plotted vs. Ra_L*/Da_L for cylinders in all sizes of packing in Figure 37 through Figure 40. Although the data points for all cylinders are close to each other, but no single equation still can represent the whole set of the data.

Data for smaller cylinders exhibit higher modified Sherwood numbers with respect to Ra_L*/Da_L. This could be explained by the effect that curvature has on the mass transfer. This was also observed in the case of cylinders in free solution. Larger diameter cylinders can be approximated by flat plate correlations

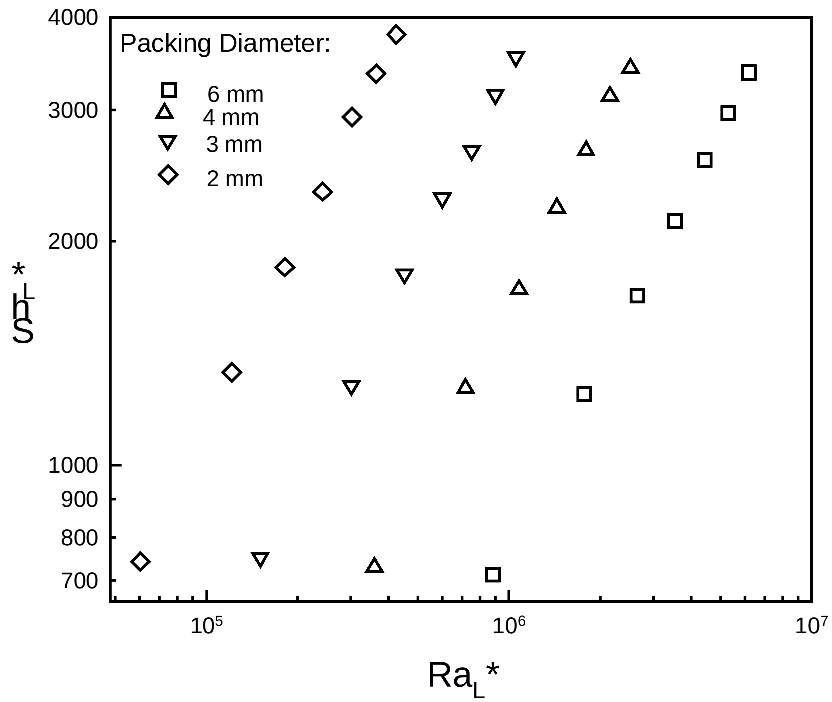

Figure 31: Average Modified Sherwood number vs. Modified Rayleigh number for Cylinder 1 in porous media

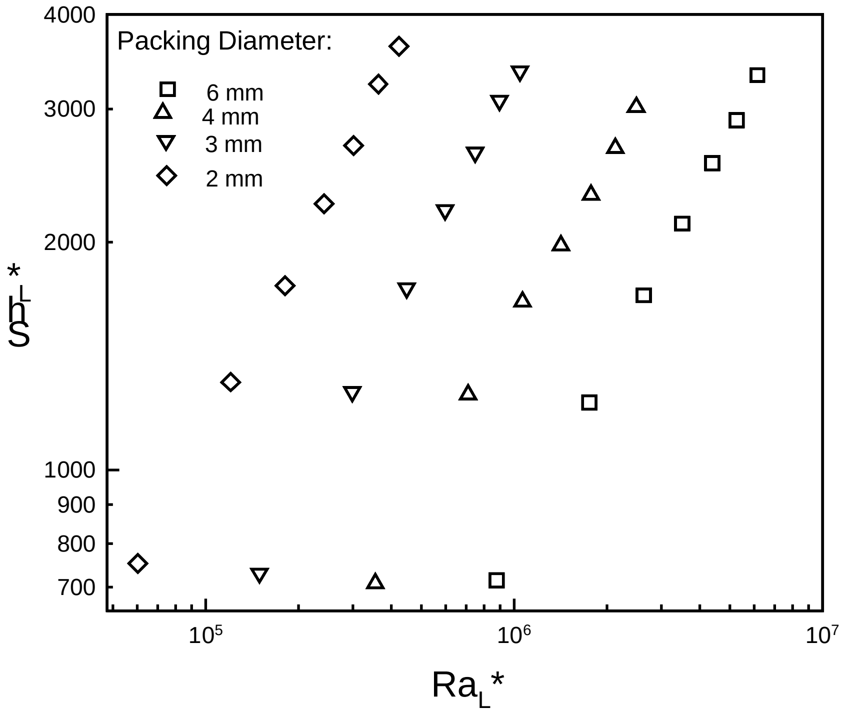

Figure 32: **Average Modified Sherwood number vs. Modified Rayleigh number for Cylinder 2 in porous media**

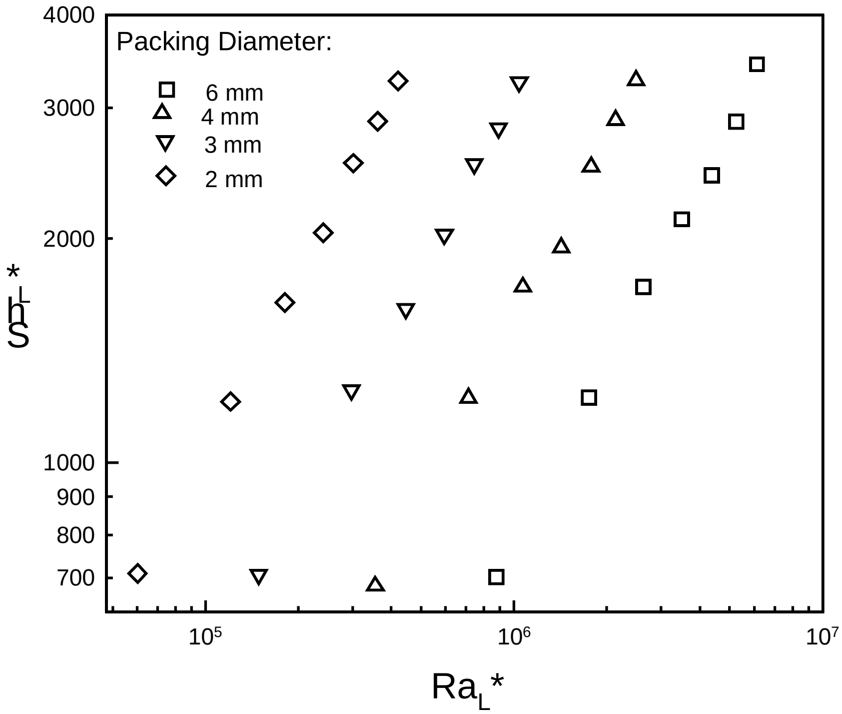

Figure 33: Average Modified Sherwood number vs. Modified Rayleigh number for Cylinder 4 in porous media

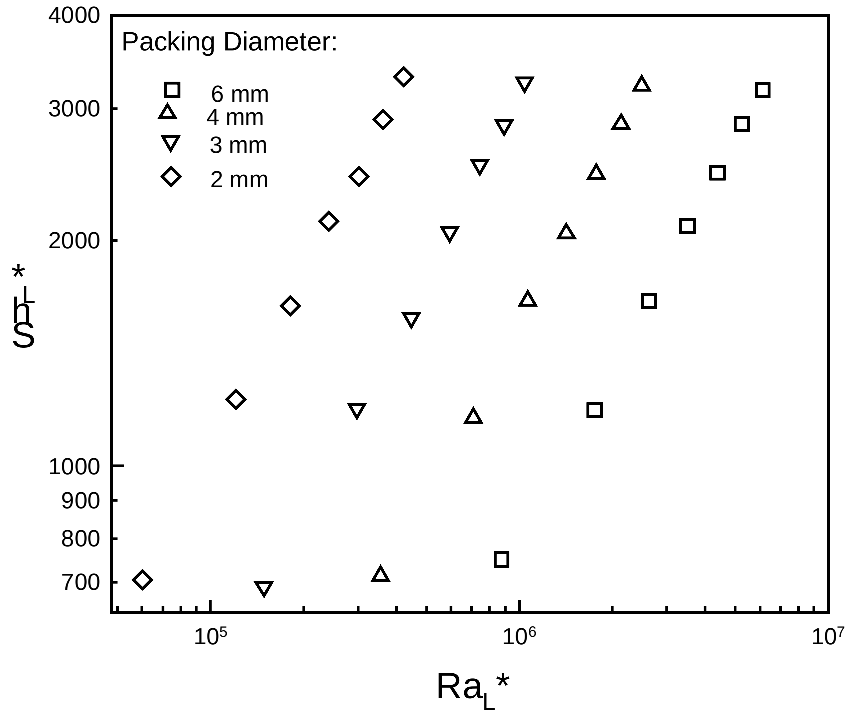

Figure 34: **Average Modified Sherwood number vs. Modified Rayleigh number for Cylinder 5 in porous media**

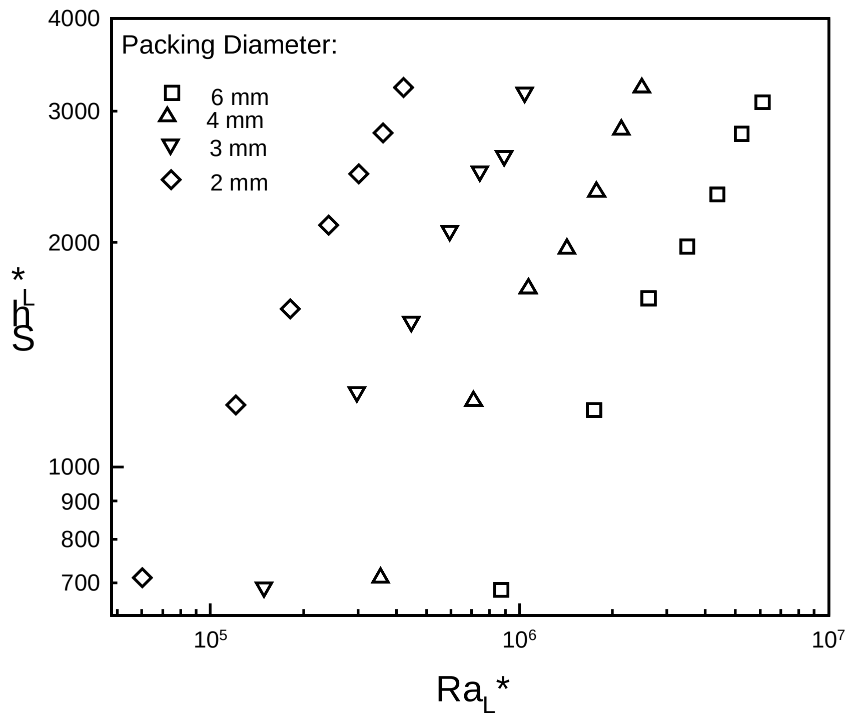

Figure 35: **Average Modified Sherwood number vs. Modified Rayleigh number for Cylinder 6 in porous media**

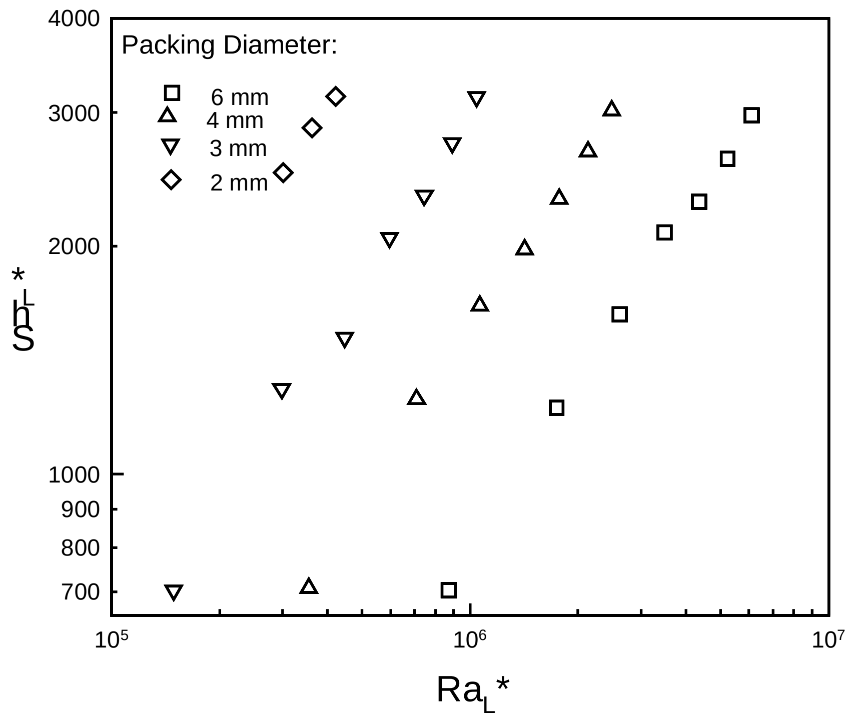

Figure 36: Average Modified Sherwood number vs. Modified Rayleigh number for Cylinder 7 in porous media

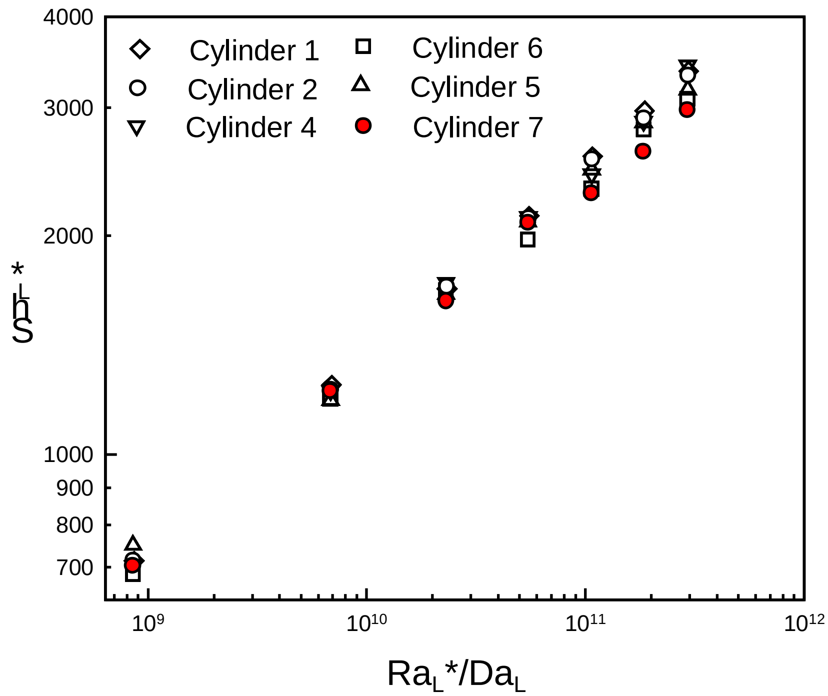

Figure 37: Average Modified Sherwood number vs. Ra_L^*/Da_L for various cylinders embedded in porous media of 6 mm diameter glass spheres

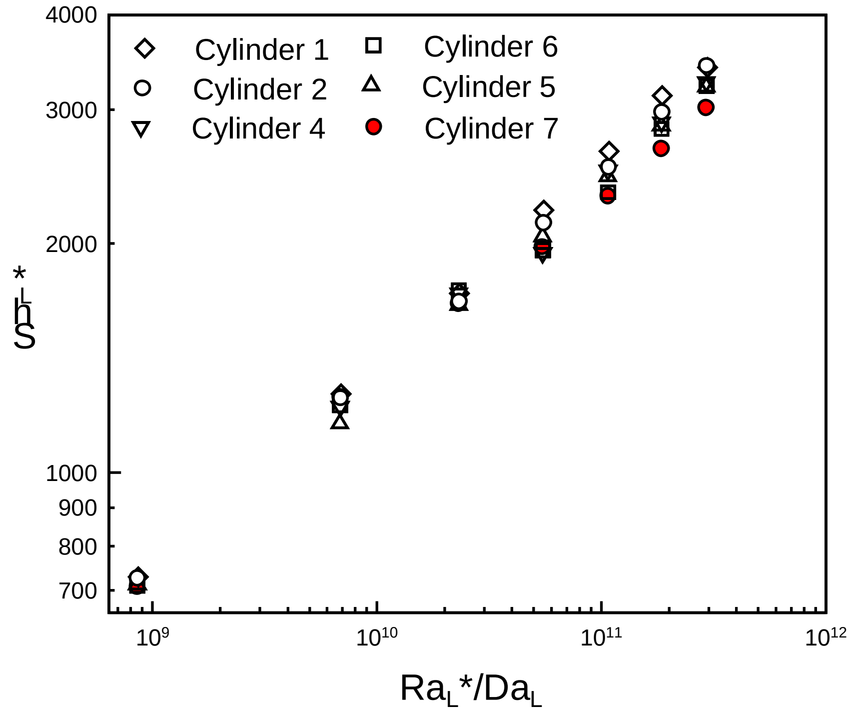

Figure 38: **Average Modified Sherwood number vs. Ra_L^*/Da_L for various cylinders in porous media of 4 mm diameter glass spheres**

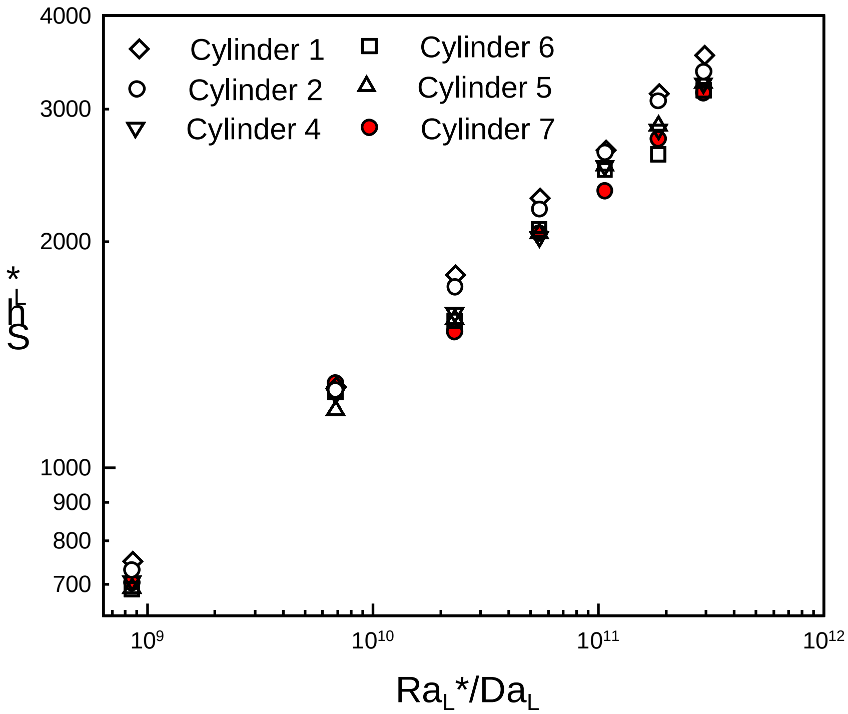

Figure 39: **Average Modified Sherwood number vs. Ra_L*/Da_L for various cylinders in porous media of 3 mm diameter glass spheres**

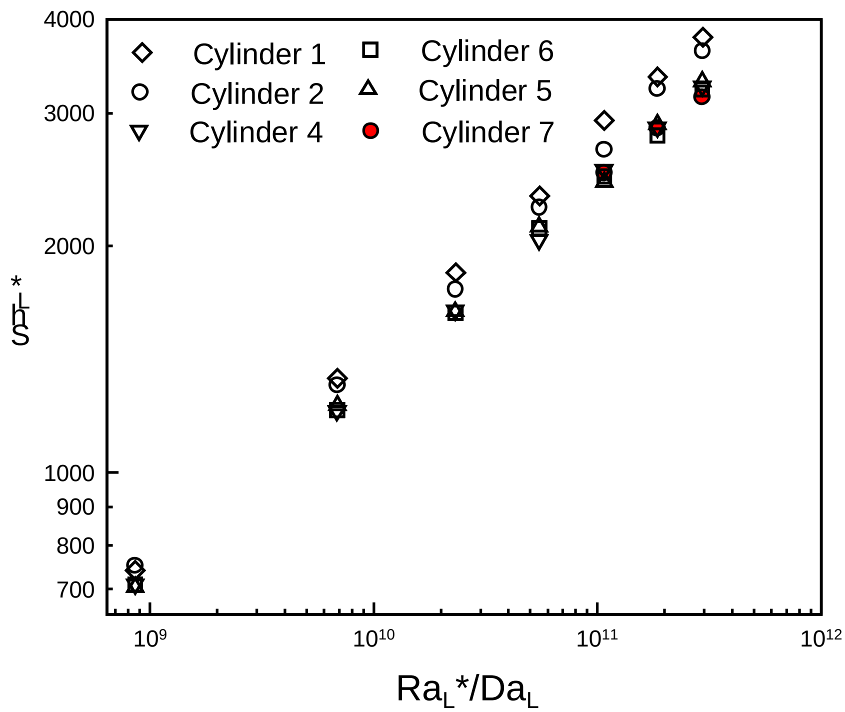

Figure 40: Average Modified Sherwood number vs. Ra_L*/Da_L for various cylinders in porous of 2 mm diameter glass spheres

Minkowycz and Cheng [21] obtained an approximate solution for the problem of natural convection about a vertical cylinder with power-law wall temperature in porous media. For a given value of the power law exponent ?p they found that the ratio of local surface heat flux of a cylinder (q_c'') to that of a flat plate (q'') is a nearly linear function of a curvature parameter ?¶:

$$\frac{q_c''}{q''} = 1 + C'?ã \quad \text{for } T_w = T_{8ã} + Ax^{?ã} \tag{34}$$

where, ?Ð= $2x/R(Ra_L^*)^{1/2}$ and C is a function of λ. For the case of constant surface temperature λ should be equal to zero. This case is analogous to constant surface concentration which represents the conditions of present experiments. Equation (34) in terms of Sherwood number can be written as:

$$Sh_L^*/Sh_L^*(Plate) = 1+C' ?x \tag{35}$$

For ?¾= 0, the value of C’ is 0.3. Using the empirical correlation for flat plate given by Rahman et al [20] given in Equation (33), the Sherwood number for the cylinders can be written as:

$$Sh_L^* = C_1\left(\frac{Ra_L^*}{Da_L}\right)^{0.26} *\left[1+\frac{0.6L}{R}(Ra_L^*)^{-0.5}\right] \tag{36}$$

Equation (45) suggests that all mass transfer data can be fitted in a straight line if Sh_L^* is plotted against $(Ra_L^*/Da_L)^{0.25} *(1+0.6L/R\ (Ra_L^*)^{-0.5})$. This is done in Figure 41, which shows a good straight line fit of slope 3.29 with $r^2 = 0.99$. The equation of the fitted line is:

$$Sh_L^* = 3.29\left(\frac{Ra_L^*}{Da_L}\right)^{0.26} *\left[1+\frac{0.6L}{R}(Ra_L^*)^{-0.5}\right] \tag{37}$$

Equation (37) can be used to predict natural convective mass transfer coefficients from vertical cylinders embedded in saturated porous media.

Table 5 shows the ranges of various parameter within which these results are expected to predict well.

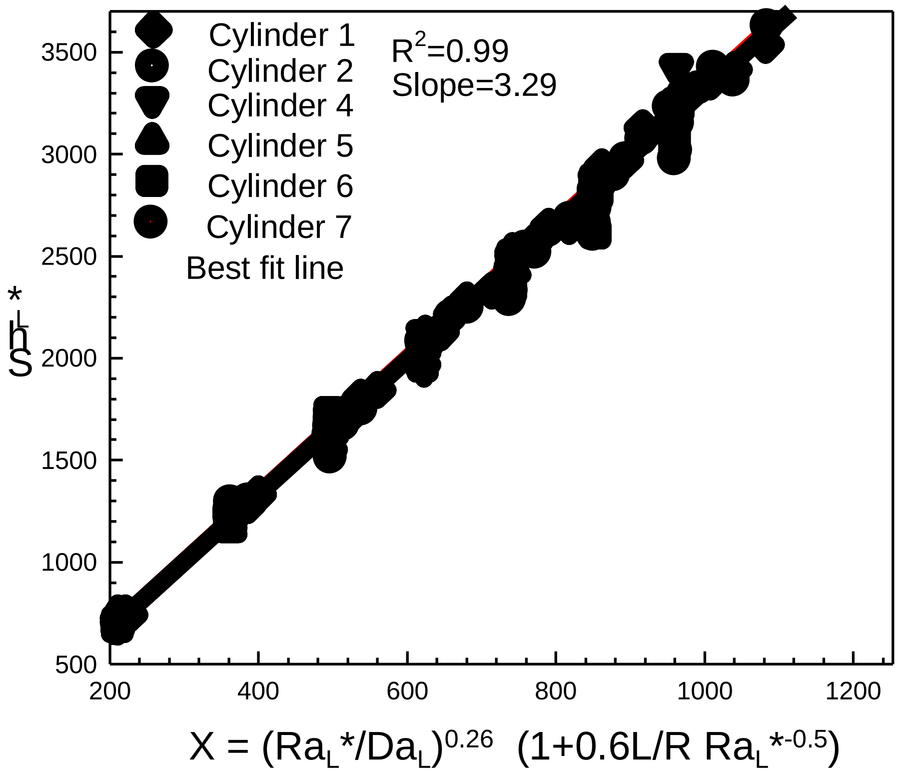

Figure 41: Sh_L* vs. $(Ra_L*/Da_L)^{0.26}$ $(1+0.6\ L/R\ Ra_L*^{-0.5})$ for cylinders in porous media of different packing sizes

Table 5: Ranges of various parameters in this study

Parameter	Range
Diameter of cylinders	0.65-28.00 mm
Height of cylinders	1.0-7.0 cm
Packing particle diameter	2.0 – 6.0 mm
Temperature	20.5 – 25.0 ºC
Ra_L^*	6×10^4 - 6.1×10^6
Da_L	1.40×10^{-6} - 1.02×10^{-3}

CHAPTER 6

CONCLUSIONS

Natural convection mass transfer coefficients from cylinders in free acidic cupric sulfate solution and in saturated porous medium, were obtained. The limiting diffusion current technique (LDCT) based on cupric ion deposition has been used. The obtained data for this geometry in quiescent solution match with those obtained in previous studies. When they are embedded in the porous media made of identical glass spheres, the mass transfer coefficient depends on the permeability. It was possible to correlate the data using modified Rayleigh number and Darcy numbers. In the studied range of the parameters, following correlations could be used to predict the mass transfer coefficients:

$$Sh_L^* = 3.29\left(\frac{Ra_L^*}{Da_L}\right)^{0.26} * \left[1 + \frac{0.6L}{R}\left(Ra_L^*\right)^{-0.5}\right] \quad \text{for embedded cylinders} \qquad (37)$$

NOMENCLATURE

A	Mass transfer area
A_1	Constant in Equation (8)
C_1 and C_2	Constants in Equation (22)
C_A	Concentration of species A
C_b	Bulk concentration of copper ions
C_s	Surface concentration of copper ions
d	Cylinder diameter
D	Molecular diffusivity of cupric ions in acidic solution
Da_L	Darcy's numbers for cylinders/plates
D_e	effective diffusivity
F	Faraday's constant
g	Acceleration due to gravity
Gr	Grashof number
$\bar{h}$	average heat transfer coefficient
I_L	limiting current
K	Permeability
k	Thermal conductivity
k_L	average mass transfer coefficient
L	Height of the cylinder/plate
Nu	Nusselt number
Pr	Prandtl number

q''	Heat flux from vertical plate
q_c''	Heat flux from cylinder
r	Radial coordinate
r_1	Concentration ratio of hydrogen and sulfate ions
R	Radius of cylinder
Ra_L	Average Rayleigh number
Ra^*_x, Ra^*_L	Modified Rayleigh number for vertical plate/cylinder
Ra^*_D	Modified Rayleigh number for horizontal cylinders
Ra	Rayleigh number defined in Equation (24)
Sc	Schmidt number
Sh_L	Average Sherwood number for vertical plate/cylinder
Sh^*_L	Average modified Sherwood number estimated for vertical plate/cylinder
Sh_{r-L}	Average Sherwood number (Equation 32)
T, T_w and $T_{8\tilde{a}}$	Temperature at wall and in bulk.
t	Transference number
x and *y*	Axial coordinates
z	Number of electrons in reduction reaction

Greek Letters

α	equal to $1/Sh_{r-L}$
α_m	Thermal diffusivity for porous media
ß.	Thermal expansion coefficient

?)	Curvature parameter defined in Equation (31)
?L	Kinematic viscosity
?þ	Density at surface
?“8ã	Dulk density
ε	Porosity
λ	A constant in Equation (7)
ξ	Curvature parameter defined in Equation (18)
θ	Dimensionless temperature
	Potential

REFERENCES

1. D. A. Nield, and A. Bejan "Convection in Porous Media" 2nd ed, Springer-Verg, New York, (1999).
2. S. H. Chan and H. Y. Chen, "Modeling of Through-Hole Electrodeposition; Part I: Effect of Electrical Migration" Journal of Applied Electrochemistry, **31**, 605, (2001).
3. I. Pop, D. B. Ingham and J. H. Merkin, "Transient Convection Heat Transfer in a Porous Medium: External Flows", in Ingham, D. B. and I. Pop. (Ed). "Transport Phenomena in Porous Media", Elsevier Science, Oxford. (1998)
4. J. R. Selman and C. W. Tobias, "Mass Transfer Measurements by Limiting Current Technique", Advanced Chemical Engineering. **10**, 211 (1977)
5. John. S. Newman, "Electrochemical Systems", 2nd ed, Prentice Hall, New Jersey, (1991).
6. H.D. Chiang and R. J. Goldstein, "Application of the Electrochemical Mass Transfer Technique to the Study of Buoyancy-Driven Flows", Proceedings of the 4th Inter. Symp. On Transport Phenomena in Heat and Mass Transfer, **1**, (1991).
7. A. A. Wragg, "Use of Electrochemical Techniques to Study Natural Convection Heat and Mass Transfer" Journal of Applied Electrochemistry, **21**, 1047 (1991).
8. C. Ponce-de-León and R. W. Field, "On the Determination of Limiting Current Density from Uncertain Data" Journal of Applied Electrochemistry, **30**, 1087, (2000).
9. P. Cheng and W. J. Minkowycz, "Free Convection About a Vertical Flat Plate Embedded in a Porous Medium with Application to Heat Transfer from a Dike" Journal of Geophysical Research, **82**, n14, 2040 (1977).
10. P. Cheng and C. T. Hsu, "High-Order Approximations for Darcian Free Convective Flow about a Semi-Infinite Vertical Flat Plate" Transactions of ASME: Journal of Heat Transfer, **106**, 143 (1984).
11. Y. Joshi and B. Gebhart, "Vertical Natural Convection Flows in Porous Media Calculations of Improved Accuracy" International Journal of Heat and Mass Transfer, **27**, n1, 69, (1984).

12. A. Bejan and D. Poulikakos, "The Non-Darcy Regime for Vertical Boundary Layer Natural Convection in a Porous Medium" International Journal of Heat and Mass Transfer, **27**, n5, 717 (1984).

13. C. T. Plumb and J. C. Huenefeld, "Non-Darcy Convection from Heated Surfaces in Saturated Porous Media" International Journal of Heat and Mass Transfer, **24**, n4, 765 (1981).

14. C. T. Hsu and P. Cheng, "The Brinkman Model for Natural Convection about a Semi-Infinite Vertical Flat Plate in a Porous Medium" International Journal of Heat and Mass Transfer, **28**, n3, 683 (1985).

15. G. H. Evans and O. A. Plumb, "Natural Convection from a Vertical Isothermal Surface Embedded in a Saturated Porous Medium" AIAA-ASME Therophysics and Heat Transfer Conference, Paper 78-HT-55. Palo Alto, California (1978).

16. S. J. Kim and K. Vafai, "Analysis of Natural Convection about a Vertical Plate Embedded in Porous Medium", International Journal of Heat and Mass Transfer, **34**, n4, 665 (1989).

17. P. Cheng, C. L. Ali and A. K. Verma, "An Experimental Study of Non-Darcian Effects in a Saturated Porous Medium" Letters on Heat and Mass Transfer, **8**, 261 (1981).

18. M. Kaviany and M. Mittal, "Natural Convection Heat Transfer from a Vertical Plate to High Permeability Porous Media: An Experiment and Approximate Solution", International Journal of Heat and Mass Transfer, **30**, n5, 967 (1987).

19. M. Kaviany and M. Mittal, "And Experimental Study of Vertical Plate Natural Convection in Porous Media", in L. S. Yao (Ed.) Heat Transfer in Porous Media and Particulate Flow, American Society of Mechanical Engineers (1965).

20. S. U. Rahman, M. A. Al-Saleh and R. N. Sharma, "An Experimental Study on Natural Convection from Vertical Surfaces Embedded in Porous Media" Industrial Engineering Chemical Resources, **39**, 214(2000).

21. W. J. Minkowycz and P. Chen, "Free Convection about a Vertical Cylinder Embedded in a Porous Medium", International Journal of Heat and Mass Transfer, **19**, 805 (1976).

22. M. J. Huang and C. K. Chen, “Effects of Surface Mass Transfer on Free Convection Flow over Vertical Cylinder Embedded in a Saturated Porous Medium”, ASME J. Energy Recourses Technology. **107**, 394 (1985).

23. S. Kimura, “Transient Forced and Natural Convection Heat Transfer about a Porous Medium”, International Journal of Heat and Mass Transfer, **33**, 617 (1989).

24. A. Yucel, “Natural Convection Heat and Mass Transfer along a Vertical Cylinder in a Porous Medium”, International Journal of Heat and Mass Transfer, **33**, n10, 2265 (1990).

25. F. C. Lai, C. Y. Choi and F. A. Kulacki, “Coupled Heat and Mass Transfer by Natural Convection from Slender Bodies of Revolution in Porous Media”, Int. Comm. Heat Mass Transfer, **17**, 609 (1990).

26. I. Pop, Tsung-Yen Na “Darcian Mixed Convection along Slender Vertical Cylinders with Variable Surface Heat Flux Embedded in a Porous Medium”, Int. Comm. Heat Mass Transfer, **25**, 251(1998).

27. T. K. Aldoss, M. A. Jarrah and B. J. Al-Sha’er, “Mixed Convection from a Vertical Cylinder Embedded in a Porous Medium: non-Darcy Model”, International Journal of Heat and Mass Transfer, **39**, n4, 1141 (1996).

28. M. Kumari and G. Nath, “Double Diffusive Unsteady Free Convection on Two-Dimensional and Axisymmetric Bodies in a Porous Medium”, International Journal of Energy Research, **13**, 379 (1989).

29. T. K. Aldoss, “MHD Mixed Convection from a Vertical Cylinder Embedded in a Porous Medium”, Int. Comm. Heat Mass Transfer, **23**, n4, 517 (1996).

30. J. H. Merkin, “Free Convection Boundary Layers in a Saturated Porous Medium with Lateral Mass Flux”, International Journal of Heat and Mass Transfer, **21**, 1499 (1978).

31. H. T. Chen, and C. K. Chen, “Natural Convection of a non-Newtonian Fluid about a Horizontal Cylinder and a Sphere in a Porous Medium”, Int. Comm. Heat and Mass Transfer **15**, 605 (1988).

32. R. M. Fand, T. E. Steinberber and P. Cheng, “Natural Convection Heat Transfer from a Horizontal Cylinder Embedded in Porous Medium”, International Journal of Heat and Mass Transfer, **29**, 119 (1986).

33. B. Farouk, and H. Shayer, “Natural Convection around a Heated Cylinder in a Saturated Porous Medium”, ASME J. Heat Transfer, **110**, 642-648, (1988).

34. R. T. Fernandez and and V. E. Schrock, “Natural Convection from Cylinders Embedded in a Liquid-Saturated Porous Medium”, Heat Transfer, Elsevier, Amsterdam, **2**, 335 (1982).

35. P. Cheng, “Mixed Convection about a Horizontal Cylinder Embedded in a Fluid-Saturated Porous Medium”, International Journal of Heat and Mass Transfer, **25**, 1245, (1982).

36. T. Sano, “Unsteady Heat Transfer from a Circular Cylinder Immersed in a Darcy Flow”, J. Eng. Math. **14**, 177 (1980)

37. D. B. Ingham, J. H. Merkin and I. Pop, “The Collision of Free-Convection Boundary Layers on a Horizontal Cylinder Embedded in a Porous Medium”, Quart. J. Mech. Appl. Math. **36**, 313 (1983).

38. I. Pop, D. B. Ingham and P. Cheng, “Transient Free Convection about a Horizontal Circular Cylinder in a Porous Medium”, Fluid Dynamics Research, **12**, 295 (1993).

39. I. Pop, D. B. Ingham and R. Bradean, “Transient Free Convection about a Horizontal Cylinder in a Porous Medium with Constant Surface Flux Heating”, Acta Mechanica, **119**, 79, (1996).

40. P. A. Tyvand, “First-Order Transient Free Convection about a Horizontal Cylinder Embedded in a Porous Medium”, Fluid Dynamics Research **15**, 277 (1995).

41. H. O. Sundfor and P. A. Tyvand, “Transient Free Convection in a Horizontal Porous Cylinder with a Sudden Change in Wall Temperature”, in: J. Grue, B. Gjevik and J. E. Weber (eds.) Waves and Nonlinear Processes in Hydrodynamics, Kluwer, Holland 291 (1996).

42. R. Bradean, D. B. Ingham, P. J. Heggs and I. Pop, “Unsteady Free Convection Adjacent to an Impulsively Heated Horizontal Circular Cylinder in a Porous Medium”, Numerical Heat Transfer, **34**, n3, 325 (1997).

43. P. Cheng, T. T. Le and I. Pop, “Natural Convection of a Darcian Fluid about a Cone”, Int. Comm. Heat Mass Transfer, **12**, 705-717 (1985).

44. I. Pop and P. Cheng, " An Integral Solution for Free Convection of a Darcian Fluid about a Cone with Curvature Effects", Int. Comm. Heat Mass Transfer, **13**, 433 (1986).

45. R. Vasantha, I. Pop and G. Nath, "Non-Darcy Natural Convection over a Slender Vertical Frustum of a Cone in a Saturated Porous Medium", International Journal of Heat and Mass Transfer, **29**, 153-156 (1986).

46. A. Nakayama, T. Kokudai and H. Koyama, "Integral Method for Non-Darcy Free Convection over a Vertical Flat Plate and Cone Embedded in a Fluid-Saturated Porous Medium", Warme-Stoffubertrag, **23**, 337 (1988).

47. K. A. Yih, "Effect of Uniform Lateral Mass flux on Free Convection about a Vertical Cone Embedded in a Saturated Porous Medium", Int. Comm. Heat Mass Transfer, **24**, n8, 1195 (1997).

48. K. A. Yih, "Coupled Heat and Mass Transfer over a Truncated Cone in Porous Media", Acta Mechanica, **137**, n1, 83 (1999).

49. K. A. Yih, "Uniform Transpiration Effect on Combined Heat and Mass Transfer by Natural Convection over a Cone in Saturated Porous Media", International Journal of Heat and Mass Transfer, **42**, n18, 3533 (1999).

50. K. A. Yih, "Uniform Lateral Mass Flux Effect on Natural Convection of non-Newtonian Fluids over a Cone in Porous Media", Int. Comm. Heat Mass Transfer, **25**, n7, 959 (1998).

51. Y. T. Yang and S. J. Wang, "Free Convection Heat Transfer of non-Newtonian Fluids over Axisymmetric and Two-Dimensional Bodies of Arbitrary Shape Embedded in a Fluid-Saturated Porous Medium', International Journal of Heat and Mass Transfer, **39**, n1, 203 (1996).

52. R. K. Tripathi, A. Sau and G. Nath, "Laminar Free Convection Flow over a Cone Embedded in a Stratified Medium", Mechanics Research Comm., **21**, n3, 289 (1994).

53. G. Ramanaiah and G. Malarvizhi, "Natural Convection Adjacent to Surfaces Embedded in Thermally Stratified Porous Media", Natural Forced Convection and Combustion Simulation, Second Int. Conf. Adv. Comput. Method Heat Transfer , Publ. By Computational Mechanics Inc., Billerica, MA, USA, 431 (1992).

54. M. M. Rahman and A. Faghri, “ Evaporation, Heating, Solid Dissolution, and Gas Absorption in a Thin Liquid Film on the Outer Surface of a Wedge or Cone Embedded in a Porous Medium”, Proceedings of the 3rd ASME/JSME Thermal Engineering Joint Conference. Publ. By ASME, NY, 233 (1991).

55. M. M. Rahman and A. Faghri, “Transport in a Thin Liquid Film on the Outer Surface of a Wedge or Cone Embedded in a Porous Medium. Part II”, Int. Comm. Heat Mass Transfer, **20**, n1, 29 (1993).

56. M. M. Rahman and A. Faghri, “Transport in a Thin Liquid Film on the Outer Surface of a Wedge or Cone Embedded in a Porous Medium. Part I. Mathematical analysis”, Int. Comm. Heat Mass Transfer, **20**, n1, 15 (1993).

57. N. G. Kafoussias, “MHD Free Convective Flow Through a non-Homogeneous Porous Medium over an Isothermal Cone Surface”, Mechanics Research comm., **19**, n2, 89 (1992).

58. A. J. Chamkha, “Non-Darcy Hydromagnetic Free Convection from a Cone and a Wedge in Porous Media”, Int. Comm. Heat Mass Transfer, **23**, n6, 875 (1996).

59. I. Pop and T. Na, “Natural Convection over a Frustum of a Wavy Cone in a Porous Medium”, Mechanics Research Comm., **22**, n2, 181 (1995).

60. Skelland A. H. P. Diffusional Mass Transfer; R. E. Krigger Publishing Company: Malabar, FL, 1985.

61. E. Ravoo, J. W. Rotte and F. W. Sevenstern, "Theoretical and Electrochemical Investigation of Free Convection Mass Transfer at Vertical Cylinders", Chemical Engineering Science, **25**, 1637 (1970)

APPENDIX A

POLARIZATION CURVES FOR VERTICAL CYLINDERS

VITA

Name:	Mubarak A. Al-Khater
Date of Birth:	February 08, 1975
Place of Birth:	Khobar, Saudi Arabia
Nationality:	Saudi
Educational Qualification:	B. S. Chemical Engineering (1997)
	King Fhad University of Petroleum & Minerals
	Dhahran 31261, Kingdom of Saudi Arabia
	M.S. Chemical Engineering (2004)
	King Fhad University of Petroleum & Minerals
	Dhahran 31261, Kingdom of Saudi Arabia
Work Experience:	Process Control Engineer (1998 to 2001)
	Al-Jubail Petrochemical Company (Kemya)
	Jubail 31961, Kingdom of Saudi Arabia
	Chemical Engineer (2001 - Recent)
	Saudi Aramco
	Dhahran 31311, Kingdom of Saudi Arabia